



Published in final edited form as:

Cancer Cell. 2018 September 10; 34(3): 513–528.e8. doi:10.1016/j.ccell.2018.08.003.

Disruption of the β 1L isoform of GABP reverses glioblastoma replicative immortality in a *TERT* promoter mutation-dependent manner

Andrew Mancini^{1,13}, Ana Xavier-Magalhães^{1,2,3,13}, Wendy S. Woods⁴, Kien-Thiet Nguyen¹, Alexandra M. Amen^{1,5}, Josie L. Hayes¹, Christof Fellmann⁵, Michael Gapinske⁴, Andrew M. McKinney¹, Chibo Hong¹, Lindsey E. Jones¹, Kyle M. Walsh⁶, Robert J.A. Bell¹, Jennifer A. Doudna^{5,7,8,9,10}, Bruno M. Costa^{2,3}, Jun S. Song^{11,12}, Pablo Perez-Pinera^{4,12}, and Joseph F. Costello^{1,14,*}

¹Department of Neurological Surgery, University of California, San Francisco, CA 94158, USA

²Life and Health Sciences Research Institute (ICVS), School of Medicine, University of Minho, 4710-057 Braga, Portugal

³ICVS/3B's-PT Government Associate Laboratory, Braga/Guimarães, 4710-057 Braga, Portugal

⁴Department of Bioengineering, University of Illinois, Urbana-Champaign, IL 61801, USA

⁵Department of Molecular and Cell Biology, University of California, Berkeley, CA 94720, USA

⁶Division of Neuroepidemiology, Department of Neurological Surgery, University of California, San Francisco, CA 94158, USA

⁷Department of Chemistry, University of California, Berkeley, CA 94720, USA

⁸Innovative Genomics Institute, University of California, Berkeley, CA 94720, USA

⁹MBIB Division, Lawrence Berkeley National Laboratory, Berkeley, CA 94720, USA

¹⁰Howard Hughes Medical Institute (HHMI), Berkeley, CA 94720, USA

¹¹Department of Physics, University of Illinois, Urbana-Champaign, IL 61801, USA

¹²Carl R. Woese Institute for Genomic Biology, University of Illinois, Urbana-Champaign, IL 61801, USA

¹³These authors contributed equally to this work.

¹⁴Lead Contact

*Correspondence: joseph.costello@ucsf.edu.

Author Contributions: Conceptualization: A.M., A.X-M., R.J.A.B. and J.F.C.; Methodology: A.M., A.X-M, CRISPR-Cas9 Methodology: W.S.W., M.G. and P.P-P., *in vivo* Methodology: K.T.N.; P278 GNS culture generation: L.E.J.; Formal Analysis: A.M., A.X-M., W.S.W., J.L.H., A.M.A.; Investigation: A.M., A.X-M., A.M.A., C.H.; Software and data curation: J.L.H.; Writing: A.M., A.X-M., R.J.A.B. and J.F.C.; Discussion: C.F., K.M.W., R.J.A.B., J.A.D., B.M.C., and J.S.S.; Supervision: J.F.C., CRISPR-Cas9 Supervision: P.P-P.; Funding Acquisition: J.F.C., J.S.S.

Publisher's Disclaimer: This is a PDF file of an unedited manuscript that has been accepted for publication. As a service to our customers we are providing this early version of the manuscript. The manuscript will undergo copyediting, typesetting, and review of the resulting proof before it is published in its final citable form. Please note that during the production process errors may be discovered which could affect the content, and all legal disclaimers that apply to the journal pertain.

Competing Financial Interests: R.J.A.B and J.F.C are co-founders of Telo Therapeutics Inc. and have ownership interest.

Summary

TERT promoter mutations reactivate telomerase, allowing for indefinite telomere maintenance and enabling cellular immortalization. These mutations specifically recruit the multimeric ETS factor GABP, which can form two functionally independent transcription factor species – a dimer or a tetramer. We show that genetic disruption of GABP β 1L (β 1L), a tetramer-forming isoform of GABP that is dispensable for normal development, results in *TERT* silencing in a *TERT* promoter mutation-dependent manner. Reducing *TERT* expression by disrupting β 1L culminates in telomere loss and cell death exclusively in *TERT* promoter mutant cells. Orthotopic xenografting of β 1L-reduced, *TERT* promoter mutant glioblastoma cells rendered lower tumor burden and longer overall survival in mice. These results highlight the critical role of GABP β 1L in enabling immortality in *TERT* promoter mutant glioblastoma.

Introduction:

Telomeres maintain DNA integrity by protecting the ends of chromosomes but progressively shorten with each cell division (Blackburn et al., 2006; Counter et al., 1992). Telomere length is maintained by telomerase, a multi-subunit complex that binds and elongates the telomere ends. Telomerase Reverse Transcriptase (TERT) is the catalytic subunit of telomerase, and its expression is the rate-limiting step in telomerase activity across a wide range of tissues (Bryan and Cech, 1999; Counter et al., 1998). While normally silenced in somatic cells, over 90% of human tumors reactivate *TERT* expression, allowing cancer cells to gain replicative immortality by avoiding cell death and senescence associated with telomere shortening (Chin et al., 1999; Kim et al., 1994; Saretzki et al., 1999; Shay and Wright, 2000). Two activating mutation hotspots in the *TERT* promoter, termed C228T and C250T, are found in over 50 tumor types, and are the most frequent mutations in several tumor types, including 83% of primary *IDH* wild-type glioblastomas (GBM) and 78% of oligodendrogliomas (Arita et al., 2013; Killela et al., 2013; Zehir et al., 2017). These mutually exclusive mutations exist predominantly in the heterozygous state, acting as the drivers of telomerase reactivation (Horn et al., 2013; Huang et al., 2013; Killela et al., 2013). In high-grade gliomas, *TERT* promoter mutations correlate with increased *TERT* mRNA levels and enhanced telomerase activity (Spiegel-Kreinecker et al., 2015; Vinagre et al., 2013). Furthermore, in tumor cells bearing *TERT* promoter mutations, these mutations are necessary – albeit not sufficient – for achieving replicative immortality (Chiba et al., 2015; Chiba et al., 2017). Both *TERT* promoter mutations generate identical 11 base pair sequences that form a *de novo* binding site for the ETS transcription factor GA-binding protein (GABP) (Bell et al., 2015). The presence of either promoter mutation allows GABP to selectively bind and activate the mutant *TERT* promoter while the wild-type allele remains silenced (Akincilar et al., 2016; Bell et al., 2015; Stern et al., 2015). GABP has no known role in *TERT* regulation outside of *TERT* promoter mutant tumors.

The GABP transcription factor is an obligate multimer consisting of the DNA-binding GABP α subunit and trans-activating GABP β subunit. GABP can act as a heterodimer (GABP $\alpha\beta$) composed of one GABP α and one GABP β subunit or a heterotetramer (GABP $\alpha_2\beta_2$) composed of two GABP α and two GABP β subunits (Rosmarin et al., 2004; Sawada et al., 1994). Two distinct genes encode the GABP β subunit, *GABPB1* encodes

GABP β 1 (β 1) and *GABPB2* encodes GABP β 2 (β 2). β 1 has two isoforms transcribed from the *GABPB1* locus, the shorter GABP β 1S (β 1S) and the longer GABP β 1L (β 1L), while β 2 has a single isoform (de la Brousse et al., 1994; Rosmarin et al., 2004). Whereas β 1S is able to dimerize only with GABP α , both β 1L and β 2 possess a C-terminal leucine-zipper domain (LZD) that mediates the tetramerization of two GABP $\alpha\beta$ heterodimers (de la Brousse et al., 1994; Rosmarin et al., 2004). Although β 1L or β 2 can form the GABP tetramer, GABP tetramers containing only the β 1L isoform are functionally distinct from β 2-containing tetramers and may control separate transcriptional programs (Jing et al., 2008; Yu et al., 2012). Furthermore, while abolishing the full tetramer-specific (β 1L and β 2) transcriptional program impairs the self-renewal of hematopoietic stem cells in mice (Yu et al., 2012), inhibition of the β 1L-only tetramer-specific transcriptional program has minimal phenotypic consequences in a murine system (Jing et al., 2008; Xue et al., 2008). Thus, if the GABP tetramer-forming isoforms are necessary to activate the mutant *TERT* promoter, disrupting the function of these isoforms may be a viable approach to selectively inhibit *TERT* and reverse replicative immortality in *TERT* promoter mutant cancer.

However, it is currently unclear whether the GABP tetramer-forming isoforms are necessary to activate the mutant *TERT* promoter or whether the GABP dimer is sufficient. Two proximal GABP α binding sites are required to recruit a GABP $\alpha_2\beta_2$ tetramer, and, interestingly, the *TERT* promoter has native ETS binding sites upstream of the hotspot mutations that are required for robust activation of the mutant promoter (Bell et al., 2015). These native ETS binding sites are located approximately three and five helical turns of DNA away from the C228T and C250T mutation sites, respectively, which is consistent with the optimal spacing for the recruitment of the GABP tetramer (Bell et al., 2015; Chinenov et al., 2000; Yu et al., 1997). Here we tested the hypothesis that the C228T and C250T hotspot promoter mutations recruit the tetramer-specific GABP isoforms to the mutant *TERT* promoter to enable telomere maintenance and replicative immortality.

Results:

The GABP tetramer-forming isoform β 1L positively regulates *TERT* expression in *TERT* promoter mutant - but not wild-type - tumor cells

To determine if the GABP dimer-forming isoform (β 1S) or the tetramer-forming isoforms (β 1L and β 2) regulate the mutant *TERT* promoter, we performed gene knockdown experiments *in vitro* and expression correlation analysis in primary tumors. We used siRNA-mediated knockdown of β 1 - affecting β 1S and β 1L - and β 2 in three *TERT* promoter mutant glioma cell lines, six early passage primary cultures and five *TERT* promoter wild-type and *TERT* expressing cell lines. Knockdown of β 1 significantly reduced *TERT* expression in eight of nine *TERT* promoter mutant cell cultures, but had limited effect in the *TERT* promoter wild-type cultures (Figure 1A). In contrast, siRNA-mediated knockdown of β 2 had a less robust and more variable effect on *TERT* expression in *TERT* promoter mutant cells (Figure S1A).

We also tested whether the expression of *TERT* correlates with expression of specific GABP isoforms in clinical samples, including *TERT* promoter mutant GBMs and oligodendrogliomas. This analysis revealed a significant positive monotonic association

between *TERT* and *GABPB1L* mRNA in both cancer types (Figure 1B), but no significant correlation between *TERT* and *GABPB1S* (Figure 1B) or *GABPB2* (Figure S1B) mRNA levels. Analysis of GABP isoform and *TERT* expression data in the predominantly *TERT* promoter wild-type colorectal cancer revealed no positive correlation between *TERT* expression and *GABPB1L* or *GABPB2* expression, although a positive correlation between *TERT* expression and *GABPB1S* expression was found (Figure S1C). Due to the significant positive correlation between *GABPB1L* expression and *TERT* expression in glioma, we specifically looked for depletion of the tetramer-forming *GABPB1L* isoform mRNA in our β 1 knockdown study and confirmed that this isoform mRNA was significantly depleted after siRNA-mediated knockdown in 13 of 14 cell lines (Figure 1C).

We further explored this potential dependence on the β 1L isoform for activation of the mutant *TERT* promoter by directly knocking down β 1L with a degradation-inducing Locked Nucleic Acid Anti-Sense Oligonucleotide (LNA-ASO) targeted to the *GABPB1L*-exclusive 3' UTR of the *GABPB1* transcript. This LNA-ASO specifically depleted *GABPB1L* transcript levels with no reduction in *GABPB1S* transcript levels (Figure S1D). LNA-ASO-mediated knockdown of β 1L reduced *TERT* expression across all *TERT* promoter mutant cultures and had no effect on *TERT* expression in all *TERT* promoter wild-type cultures (Figure 1D). Taken together, these data support that the GABP tetramer-forming isoform β 1L positively regulates *TERT* expression in *TERT* promoter mutant glioma.

CRISPR-Cas9-mediated disruption of *GABPB1L* reduces GABP-mediated activation of the mutant *TERT* promoter

We then directly tested the necessity of β 1L for mutant *TERT* promoter activation by generating clones with reduced β 1L function from three of the aforementioned *TERT* promoter mutant GBM cell lines (GBM1, T98G, and LN229) and three *TERT* promoter wild-type control cell lines (NHAPC5, HCT116 and HEK293T) using nuclease-assisted vector integration (NAVI) CRISPR-Cas9 editing (Brown et al., 2016; Gapinske et al., 2018) (Figure 2A). We isolated two independent *GABPB1L*-edited clones (C1 and C2) and one isogenic CRISPR control clone (CTRL) for each parental line using one of two non-overlapping sgRNAs targeting *GABPB1* exon 9 or a sgRNA targeting an intergenic region of chromosome 5, respectively (Figure S2A and Table S1). *GABPB1* exon 9 contains the coding sequence for the LZD, and disruption of this exon is sufficient for ablation of the β 1L-containing tetramer while leaving β 1S intact (Chinenov et al., 2000; Sawada et al., 1994). Each *GABPB1L*-edited clone had the disruption of at least one allele via integration of a puromycin or hygromycin resistance cassette with most remaining *GABPB1L* alleles containing indels in the LZD (Figure S2B and Table S2). Analysis of cassette integration and locus integrity at predicted off-target cutting sites in coding regions (Hsu et al., 2013) via PCR and Surveyor assay, respectively, showed no aberrations outside the target regions (Figures S3A–F). *GABPB1L*-edited clones had reduced β 1L protein levels with no measurable reduction in β 1S levels, further confirming the specificity of our editing approach (Figure S3G).

We next examined whether the indels in the remaining *GABPB1L* alleles (Figure S2B) were sufficient to generate β 1L protein with reduced tetramerization activity. Using PCR-

mediated site-directed mutagenesis, we replicated three mutations (Table S3) in *GABPB1L* and assayed the ability of the mutant β 1L to form the GABP tetramer (Figure 2B). DEL1 and DEL2 are in-frame deletions in the *GABPB1L* LZD-coding region and DEL3 is a putative loss-of-function frame-shift mutation in the same domain (Figure S2B). Each of the tested mutations reduced the ability of β 1L to form the tetramer compared to the wild-type control, thereby indicating that the CRISPR-Cas9-induced mutations in the *GABPB1L* LZD-coding region are sufficient to produce variants of the GABP tetramer-forming isoform β 1L with reduced function. Thus, all *GABPB1L*-edited clones will be referred to as “ β 1L-reduced” to encompass reductions in both protein levels and protein function.

Chromatin immunoprecipitation of GABP followed by quantitative PCR (qPCR) at the mutant *TERT* promoter revealed the loss of GABP binding in the β 1L-reduced *TERT* promoter mutant clones compared to the control lines (Figure 2C). Furthermore, analysis of *TERT* expression via RT-qPCR confirmed a significant reduction in - but not complete loss of - *TERT* mRNA across all *TERT* promoter mutant clones, whereas no decreases in expression were detected in clones from *TERT* promoter wild-type cells (Figure 2D). Additionally, overexpression of exogenous β 1L in each β 1L-reduced clone was sufficient to rescue both *TERT* expression (Figures 2E and S3H) and GABP binding at the mutant *TERT* promoter (Figure 2F). Taken together, these data confirm that the GABP tetramer-forming isoform β 1L is necessary for the complete activation of the mutant *TERT* promoter.

β 1L-mediated activation of the mutant *TERT* promoter is required for telomere maintenance in GBM

As *TERT* expression is closely linked to telomere maintenance, we next investigated the effects of reducing β 1L function on telomere length in the *TERT* promoter mutant cell lines. Measurements of mean relative telomere length at four time points following CRISPR-Cas9 editing uncovered significant telomere loss only in clones from *TERT* promoter mutant cells with reduced β 1L function and *TERT* expression (Figure 3A). Expression of exogenous β 1L or *TERT* was sufficient to halt this telomere loss in all clones (Figure 3B). Uncontrolled telomere shortening and uncapping can result in end-to-end fusions of telomere-deficient chromosomes and the formation of chromatin bridges (Capper et al., 2007; der-Sarkissian et al., 2004; Hackett et al., 2001). We identified chromatin bridges in a significant proportion of the *TERT* promoter mutant, but not *TERT* promoter wild-type, β 1L-reduced clones 70–75 days after editing, indicating widespread telomere dysfunction following telomere loss (Figures 3C and S4A). Likewise, telomere dysfunction was readily rescued by expression of exogenous β 1L or *TERT* (Figures S4B and S4C). These data support that disrupting β 1L function is sufficient to induce telomere loss and dysfunction in a *TERT* promoter mutation-dependent manner.

Disrupting β 1L function is sufficient to induce short-term and long-term growth defects in *TERT* promoter mutant lines *in vitro*

Previous studies have reported that *TERT* depletion and telomere dysfunction result in both immediate and long-term growth defects (Cao et al., 2002; Fitzgerald et al., 1999; Iwado et al., 2007; Shay and Wright, 2006). Thus we sought to determine whether reduction of β 1L results in a growth phenotype as a result of reduced expression from the mutant *TERT*

promoter. Monitoring cell growth prior to significant telomere loss (days 45–48 post-editing) revealed a growth defect in all *TERT* promoter-mutant β 1L-reduced clones (Figure S5A). We further inhibited β 1L in the β 1L-reduced lines with an LNA-ASO to deplete any residual β 1L function and observed no further changes in cell growth (Figure S5B) or *TERT* expression (Figure S5C) regardless of *TERT* promoter status. Interestingly, LNA-ASO-mediated knockdown of β 1L in *TERT* promoter mutant control lines significantly reduced cell growth compared to the LNAASO controls, suggesting a short-term growth effect following reduction of β 1L and TERT levels.

Long-term changes in growth and cell viability may occur due to telomere dysfunction in the *TERT* promoter mutant, β 1L-reduced clones. We monitored each β 1L-reduced line throughout the process of telomere loss and identified a progressive loss of cell viability in β 1L-reduced clones from *TERT* promoter mutant cells, a phenotype that was absent in the clones from *TERT* promoter wild-type cells (Figure 4A). We observed complete growth arrest in both GBM1 β 1L-reduced clones, and substantial but incomplete arrest of the cultures of T98G and LN229 clones. β 1L-reduced clones derived from T98G underwent complete growth arrest in all cases except one instance when a surviving population emerged following long-term culture. Unlike GBM1 and T98G cells, both LN229 clones consistently had a population of viable cells emerge following the period of massive cell death. The underlying cause of this heterogeneity in cellular response among the three lines is unknown, but could reflect residual function of β 1L in β 1L-reduced clones, potential β 1L-independent mechanisms of activation of the mutant *TERT* promoter, or other factors. Importantly, overexpression of either exogenous β 1L or TERT was sufficient to counteract the loss of viability (Figure 4B). This gradual loss of viability signified the loss of replicative immortality in *TERT* promoter mutant β 1L-reduced clones.

β 1L regulates a subset of GABP transcription factor targets in GBM cells

We next explored whether the observed changes in growth rate and cell viability are sole consequences of TERT depletion, are mediated by changes in levels of GABP target genes, or are a combination of both factors. The four targets selected for preliminary expression analysis (*COXIV*, *EIF6*, *RPS16*, and *TFB1M*) are essential for cell growth and have been previously identified to recruit the β 1L-containing GABP tetramer via two ETS binding sites in their promoter (Carter and Avadhani, 1994; Donadini et al., 2006; Genuario and Perry, 1996; Yang et al., 2014). *SKP2* contains only one ETS binding site in its promoter and should be unaltered by changes in β 1L (Yang et al., 2007). We identified minimal differences in the expression of each of the five targets between the CRISPR control and β 1L-reduced clones (Figure 5A).

To further interrogate the effects of β 1L reduction on global gene expression, we performed RNA sequencing (RNA-seq) for our *TERT* promoter mutant CRISPR control and β 1L-reduced lines 45 days post-editing (Figure 5B and Table S4). We identified 161 transcripts, including *TERT*, differentially expressed (DE; FDR<0.05) after β 1L reduction that were common to all three *TERT* promoter mutant lines. A majority of these DE transcripts (55%) were transcribed from genes with GABP-bound promoters, as determined from ENCODE ChIP-seq data from *TERT* promoter wild-type and mutant cancer cell lines (see STAR

Methods). Interestingly, however, the vast majority (99%) of GABP-bound genes were not differentially expressed between the control and β 1L-reduced lines. Gene ontology analysis of these DE transcripts identified enrichment in genes involved in development, cell-to-cell signaling, and proliferation (Figure 5C and Table S5). This global transcriptional analysis further validates that we have significantly inhibited the function of β 1L in the β 1L-reduced cell lines. These data, in combination with our qPCR analysis of canonical GABP tetramer targets, supports previous studies delineating specific transcriptional programs that different GABP species may control (Jing et al., 2008; Xue et al., 2008; Yu et al., 2012). The basis for the differential sensitivity between the effects of disrupting β 1L function on the mutant *TERT* promoter and selected down-regulated GABP loci relative to other GABP targets is unknown, but may be due to compensation by β 1S, β 2, or other ETS factors at certain GABP binding sites and not at other sites, or due to cell type specific differences in the GABP transcriptional program. These data suggest that the GABP binding site created by mutations in the *TERT* promoter and a subset of GABP binding sites are more sensitive to inhibition of the β 1L-containing GABP tetramer, while other GABP-bound sites are less sensitive.

β 1L-reduced GBM lines accrue DNA damage and undergo mitotic cell death in a *TERT* promoter mutation-dependent manner

The direct correlation between telomere shortening and viability loss (Figure S6A) suggested that the loss of viability is a consequence of cell death or senescence induced by telomere dysfunction. The formation of chromatin bridges after telomere dysfunction induces breakage-fusion-bridge cycles that lead to the accrual of significant DNA damage in telomere-deficient cells (der-Sarkissian et al., 2004; Hackett et al., 2001). While canonical apoptosis and cellular senescence have been widely observed as results of significant DNA damage after telomere dysfunction, both mechanisms are dependent on functional p53 and RB pathways (Saretzki et al., 1999; Whitaker et al., 1995). However, these two pathways are commonly mutated in *TERT* promoter mutant GBM, including the GBM1, T98G, and LN229 lines (Table S6), making apoptosis and senescence unlikely to occur at high levels. In p53- and RB-deficient cells, mitotic cell death has been implicated as a primary phenotype following telomere dysfunction (Fragkos and Beard, 2011; Hayashi et al., 2015). Mitotic cell death can result from chromosome fusions, high-level chromosomal rearrangements and DNA damage, oft-described consequences of breakage-fusion-bridge cycles during telomere dysfunction (Hayashi et al., 2015; Vakifahmetoglu et al., 2008; Vitale et al., 2011).

Indeed, we observed a significant increase in the amount of the DNA damage marker γ -H2AX exclusive to the β 1L-reduced clones from *TERT* promoter mutant cells by day 73 post-editing (Figures 6A and S6B). Likewise, we identified giant cell micronucleation, a prominent feature of mitotic cell death (Ianzini and Mackey, 1997; Vakifahmetoglu et al., 2008), in β 1L-reduced, *TERT* promoter mutant – but not wild-type – cells at this same time point (Figures 6B and S6C). Overexpression of exogenous β 1L or *TERT* was sufficient to fully rescue both the DNA damage (Figure S7A) and mitotic cell death phenotypes (Figure S7B). Additionally, chromatin bridge formation, γ -H2AX staining, and giant cell micronucleation accumulated over three time points (days 45, 61, and 73 post-editing) in the

LN229 β 1L-reduced clones, thus supporting that these phenotypes may be dependent on telomere shortening (Figure S7C).

Moreover, cell cycle analysis of the β 1L-reduced *TERT* promoter mutant cells between day 70 and day 80 post-CRISPR-Cas9 editing revealed a modest G_2/M enrichment, another hallmark of cells undergoing mitotic cell death (Deeraksa et al., 2013) (Figures 6C and 6D). Cytometric analysis of senescence and apoptosis/necrosis markers identified a modest increase in apoptosis in *TERT* promoter mutant β 1L-reduced clones, thereby implicating non-apoptotic mitotic cell death, with modest contributions from canonical apoptosis, as the primary driver of cell death in these lines (Figure S7D). Therefore, *TERT* promoter mutation-dependent telomere dysfunction induced by reducing the function of the GABP tetramer-forming isoform β 1L and reducing *TERT* expression culminates in a loss of replicative immortality characterized by a profound loss of cell viability primarily driven by a mitotic cell death mechanism.

Reducing β 1L function impairs tumor growth and extends mouse survival *in vivo*

In order to determine the effects of β 1L disruption in a *TERT* promoter mutant setting *in vivo*, we orthotopically injected CRISPR control or β 1L-reduced LN229 cells expressing luciferase into nude mice and monitored tumor engraftment and growth via bioluminescence imaging (BLI). A proportion of the mice injected with β 1L-reduced tumor cells did not show evidence of tumor formation over the time course, and those that did form tumors showed significantly decreased tumor growth when compared to mice injected with control cells (Figures 7A and 7B). Importantly, mice injected with the control lines had a significantly shorter median survival compared to mice bearing the β 1L-reduced lines (Figure 7C). All mice were validated for tumor burden post-mortem via visual inspection. Despite LN229 C1 and C2 having an attenuated growth arrest phenotype compared to the other lines (Figure 4A), β 1L disruption and reduced *TERT* expression in these lines were sufficient to significantly inhibit tumor formation and growth and extend survival in mice injected with them. Furthermore, lentiviral transduction of LN229 C1 and C2 with a *TERT* expression vector was sufficient to rescue both the tumor growth and survival phenotypes in an independent cohort (Figures 7D–F). In conclusion, inhibition of the mutant *TERT* promoter through disrupting β 1L function is sufficient to prolong survival in mice bearing LN229 GBM xenografts.

Discussion:

Telomerase reactivation occurs in more than 90% of human cancers and is fundamental for tumor cell immortalization. While the occurrence of *TERT* promoter mutations early in GBM evolution suggests they are important for tumorigenesis, their role in maintaining telomere length, replicative immortality, and cell viability at later time points has been relatively unexplored. We have identified the tetramer-forming β 1L isoform of GABP to be a necessary component for full activation of the mutant *TERT* promoter and replicative immortality in *TERT* promoter mutant, but not wild-type, GBM cells. These results add to recent studies showing that *TERT* promoter mutations are necessary but not sufficient for cellular immortalization in *TERT* promoter mutant tumor cells (Chiba et al., 2017; Li et al.,

2015). Our results also suggest binding of the β 1L-containing GABP tetramer to the mutant *TERT* promoter is necessary to maintain maximal expression of *TERT*.

Telomere shortening and loss of cellular proliferation has been previously observed in brain tumor cultures after sustained inhibition of telomerase (Barszczyk et al., 2014; Castelo-Branco et al., 2011; Marian et al., 2010). One difference with these studies and ours is that in addition to potentially reducing the expression of *TERT*, our β 1L-reduced clones had concomitant deregulation of a subset of GABP-regulated genes that may influence the observed *TERT*-dependent phenotypes. Although overexpression of exogenous *TERT* rescued cell growth of the cells with reduced β 1L function, expression of *TERT* at more physiologic levels through activation of the endogenous wild-type *TERT* allele may allow for more precise analysis of phenotypes. Thus, we cannot fully rule out that other β 1L target genes may contribute to the *in vitro* and *in vivo* phenotypes we observed.

The growth decrease occurring as early as 48 hr after LNA-ASO-mediated knockdown of β 1L raises the possibility that, in addition to the gradual and protracted loss of viability, β 1L and *TERT* reduction also could have immediate effects. As telomere length is heterogeneous within tumor cell cultures (der-Sarkissian et al., 2004; Wang et al., 2013), cells with shorter telomeres may be more vulnerable upon reduction in *TERT* expression. Conversely, we expect that the subset of GBM cells with longer telomeres – and not those with critically short telomeres – would preferentially survive through the cell expansion required to establish the clonal cultures of β 1L-reduced cells, and then succumb to gradual decreases in telomere length at later time points. Overall this ongoing process could contribute to the gradual loss of viability detected in the bulk population assays. The more immediate effect in our LNA-ASO cell experiments is consistent with an acute telomere-mediated cell death phenotype in *NRAS*-mutant melanoma due to dependence on *TERT* expression from the mutant promoter (Reyes-Uribe et al., 2018). However, due to the limitations of our CRISPR-Cas9 experimental design and focus on later time points, further studies to investigate the mechanism of immediate cellular effects following reduction - or elimination - of β 1L function in *TERT* promoter mutant GBM will require inducible systems and single-cell analysis.

β 1L tetramerization activity and *TERT* expression were reduced but not eliminated in our experiments. Attempts to further suppress *TERT* mRNA expression in the β 1L-reduced clones through LNA-ASO-mediated knockdown of β 1L had no effect. Therefore, a low level of expression of *TERT* from the mutant promoter may be maintained independent of β 1L function. Although our data strongly support β 1L as the main driver of *TERT* expression from the mutant promoter and the primary factor enabling cell immortality in *TERT* promoter mutant GBM, they also support the existence of a secondary mechanism contributing to the overall *TERT* expression level in *TERT* promoter mutant tumor cells. Secondary mechanisms could involve an activating structural change in the mutant *TERT* promoter G-quadruplex or activation through recruitment of other ETS factors (Chaires et al., 2014; Li et al., 2015; Lim et al., 2010; Makowski et al., 2016). Additionally, the GABP tetramer-forming isoform β 2 may be able to partially activate *TERT* expression at the mutant *TERT* promoter. β 2 knockdown significantly reduced *TERT* expression levels in a subset of *TERT* promoter mutant GBM lines. However, the absence of a positive correlation

between *GABPB2* and *TERT* expression levels in glioma tissue samples and the near total loss of the occupancy of GABP at the mutant *TERT* promoter after disruption of $\beta 1L$ suggest that $\beta 2$ plays a more minor role, at least when $\beta 1L$ is present. We cannot however exclude the possibility that $\beta 2$ plays a role in regulating the mutant *TERT* promoter in a small subset of cells. Therefore, to fully eliminate *TERT* expression in *TERT* promoter GBM, it may be necessary to jointly inhibit $\beta 1L$ alongside one or more secondary mechanisms of *TERT* expression.

Overall, the present study gives credence to $\beta 1L$ as a potential therapeutic target for tumor cells with the mutant *TERT* promoter. GABP is recruited to the mutant *TERT* promoter in multiple cancer types (Akincilar et al., 2016; Bell et al., 2015; Stern et al., 2015). The prevalence of identical *TERT* promoter mutations across a large number of cancer types (Bell et al., 2016; Zehir et al., 2017) highlights the potentially widespread role of the $\beta 1L$ -containing GABP tetramer as a dominant factor responsible for enabling replicative immortality in cancer. This is particularly relevant as direct telomerase inhibitors block tumor cell immortality, but can also affect *TERT* in normal stem and germ cells (Jager and Walter, 2016; Shay and Wright, 2006). Although GABP is a transcription factor, it is an intriguing target due to its dual function as a dimer and tetramer. $\beta 1L$ is not required for normal development in mice, and in GBM cells the majority of GABP target genes do not seem to be as sensitive to reduction of $\beta 1L$ compared to the mutant *TERT* promoter. Thus, inhibiting the dispensable tetramer-forming $\beta 1L$ isoform while leaving the dimer and other cell-essential GABP isoforms unperturbed could be a viable strategy to block cellular immortality in *TERT* promoter mutant tumors, including glioma.

Star Methods:

Contact for reagent and resource sharing

Further information and requests for resources and reagents should be directed to and will be fulfilled by the Lead Contact, Joseph F. Costello (joseph.costello@ucsf.edu).

Experimental model and subject details

Cell lines and primary cell cultures—GBM1 (male), T98G (male), LN229 (female), and LN18 (male) cells were cultured in DMEM/Ham's F-12 1:1 media, 10% FBS, 1% Penicillin/Streptomycin. The GBM1 primary culture was previously described in Bell et al. 2015 (Bell et al., 2015). HEK293T (female) and NHAPC5 (male) cells were cultured in DMEM H-21 media, supplemented with 10% FBS, 1% Non-Essential Amino Acids, 1% Glutamine and 1% Penicillin/Streptomycin. The NHAPC5 culture was previously described in Ohba et al. 2016 (Ohba et al., 2016). HCT116 cells (male) were cultured in McCoy's 5A media supplemented with 10% FBS and 1% Penicillin/Streptomycin.

SF7996 (male; passage 6), SF8249 (male; passage 4), SF8279 (male; passage 4), SF9030 (male; passage 3), and SF11411 (female; passage 4) are *TERT* promoter-mutant, *IDH1*-wild-type patient-derived early passage glioma neurosphere (GNS) GBM cultures and were previously described in Fouse et al. 2014 (Fouse et al., 2014). SF7996 (GNS) and GBM1 (serum) are derived from the same piece of tumor tissue from one patient and differ only in

derivation conditions. SF10417 (male; passage 9) is a *TERT* promoter-mutant, *IDH1*-mutant patient-derived early passage recurrent high-grade GNS oligodendroglioma culture. hNPCs (male) are human Neural Precursor Cells derived from human induced pluripotent stem cells as previously described (Xu et al., 2016). All GNS cells and hNPCs were cultured in Neurocult NS-A (Stem Cell Technologies) supplemented with 2 mM L-Glutamine, 1% Penicillin/Streptomycin, B-27 without vitamin A (Invitrogen), N2 supplement, 20 ng/mL EGF, and 20 ng/mL bFGF, and 1% sodium pyruvate. SF10417 was additionally supplemented with 20 ng/mL PDGF-AA. hNPCs were additionally supplemented with 5 ng/mL heparin. Cells were grown on 1.6 $\mu\text{g}/\text{cm}^2$ laminin-coated flasks and dissociated with StemPro Accutase (Gibco). All cells were maintained at 37° Celsius, 5% CO₂. LN229, T98G, HEK293T, LN18 and HCT116 were acquired from ATCC through the UCSF Cell Culture Facility and validated for cell identity via STR testing. The GBM1, SF7996, SF8249, SF8279, SF9030, SF11411, and SF10417 cells are patient-derived cultures validated to be tumor by exome-seq and/or RNA-seq. hNPCs (Xu et al., 2016) were a generous gift from Haoqian Xu and Michael Oldham at University of California, San Francisco. All cells tested negative for mycoplasma contamination.

Animals

Mice and Animal Housing: Athymic (*nu/nu*) female mice at 5 weeks of age were purchased from Simonson Laboratories (Figures 7A–C) and Harlan Laboratories (Figures 7D and E). Five mice were grouped per cage. Humane endpoints for sacrifice were established as >15% body weight loss from last weighing and/or the presence of gross neurological symptoms such as hunching, asocial behavior, or spastic behavior. All protocols regarding animal studies were approved by the UCSF Institutional Animal Care and Use Committee (IACUC; protocol AN111064-03B) for Dr. Theodore Nicolaides at the University of California, San Francisco.

Orthotopic xenografting and *in vivo* imaging: 144 hr prior to orthotopic xenografting, LN229 control and β 1L-reduced lines were stably transduced with Firefly Luciferase Lentifect™ Purified Lentiviral Particles catalog # LPPFLUC-Lv105 (Genecopoeia) with MOI=5. Separately, 240 hr prior to orthotopic xenografting, LN229 control and β 1L-reduced lines were stably transduced with either EF1a-TERT-RFP-Bsd catalog # LV1131-RB (GenTarget) or EF1a-empty-RFP-Bsd catalog # LVP-427 lentiviral particles with MOI=0.5. Transduced cells were selected in 5 $\mu\text{g}/\text{mL}$ blasticidin (Sigma-Aldrich) for 72 hr, validated for *TERT* and *RFP* expression via RT-qPCR and fluorescent imaging, respectively, and stably transduced with Firefly Luciferase Lentifect™ Purified Lentiviral Particles catalog # LPP-FLUC-Lv105 (Genecopoeia) with MOI=5. All cells were verified for stable luciferase expression prior to injection. 30,000 LN229 CRISPR control or β 1L-reduced cells 51 days post-editing per mouse (CTRL=12 mice; C1=12 mice; C2=10 mice) or 50,000 LN229 stably transduced TERT (T) or empty vector (V) CRISPR control or β 1L-reduced cells (7 mice per group) were injected into the frontal cortex. Animal's body weight was measured 3 times per week, tumor size via bioluminescent imaging (BLI) on a Xenogen IVIS Spectrum Imaging System was evaluated 2 times per week, and general behavior and symptomatology was evaluated daily. All BLI images were taken with small binning and a

normalized exposure of 30 s recorded 12 min after intraperitoneal injection of 5 $\mu\text{L/g}$ of 30 mg/mL D-Luciferin catalog # LUCK-100 (GoldBio).

Method details

TCGA expression data set—The collection of the data from The Cancer Genome Atlas (TCGA) (Cancer Genome Atlas Research, 2008) was compliant with all applicable laws, regulations, and policies for the protection of human subjects, and necessary ethical approvals were obtained. Analysis of all data analysis was done in R project version 3.3.2 (<http://www.r-project.org/>). RSEM normalized RNA-seq expression data for GABP isoforms (GABPA: uc002yly; GABPB1S: uc001zyc, uc001zyd, uc001zye, uc001zyf; GABPB1L: uc001zya, uc001zyb; GABPB2: uc001ewr, uc001ews, uc001ewt) and *TERT* were downloaded along with clinical information from TCGA (level 3 normalized data, December 2015, <http://tcga-data.nci.nih.gov/tcga/dataAccessMatrix.htm>) for 143 GBM (109 *TERT*-expressing and 34 *TERT*-non-expressing) samples, 49 oligodendroglioma (49 *TERT* promoter-mutant samples), and 249 colorectal cancer (249 *TERT*-expressing) samples. *TERT* mutation status was obtained, when available, from Ceccarelli et al for the glioma samples (Ceccarelli et al., 2016). GABP isoforms were analyzed for monotonic associations with *TERT* using Spearman's correlation. H_0 : Spearman's $Rho=0$; H_1 : Spearman $Rho > 0$; $\alpha=0.05$. A linear trend-line was generated using the PCA orthogonal regression line.

Transcriptome sequencing and analysis—Total cellular RNA was isolated from GBM1, T98G, and LN229 CRISPR control and β1L -reduced clones 45 days post-editing via standard TRIzol protocol (ThermoFisher). Prior to library synthesis, RNA was treated with DNase (Roche), scored on an Agilent 2100 Bioanalyzer for quality control, and quantified on a Qubit® Fluoremeter using the Qubit RNA HS Assay kit (ThermoFisher). Only the samples with RIN >7 were used for RNA-seq. RNA-seq libraries were prepared with the KAPA Stranded mRNA-Seq kit for Illumina platforms (KAPA Biosystems) according to manufacturer's instructions. Briefly, 1 μg RNA was used for mRNA capture. After fragmentation, first strand synthesis, second strand synthesis, and A-tailing, Illumina adaptors with dual indexes were ligated. The libraries were amplified 11 cycles before pooling with 8–10 samples/lane for sequencing. All libraries were sequenced at the UCSF Center for Advanced Technology on an Illumina HiSeq4000 sequencer with paired-end reads and an average read length of 50 base pairs.

Adapter and polyA sequences were removed from reads using cutadapt v1.8.1, with the minimum overlap between adapter and the 3' of the read set to 1 nt. Reads shorter than 20 nts after adapter trimming were discarded. Reads were aligned with TopHat (v2.0.14) using a GENCODE V19 transcriptome-guided alignment with parameters `-r 200 -library-type fr-firststrand, --pre-filter-multihits genome`. To estimate transcript abundance, aligned data was processed with FeatureCounts (v1.4.6) with parameters `-s 2 -B -p -O -T 24` using a GENCODE V19 GTF reference.

EdgeR was used to determine differential expression between the six β1L -reduced clones and three CRISPR control clones from *TERT* promoter mutant lines. All three CRISPR control clones were used as a reference (“REF”) in comparison to the six β1L -reduced

clones (“TEST”). Genes with <1cpm/3 samples were discarded from the analysis prior to library size calculation. The Beyer-Hardwick Method was used to determine genes significantly altered between the “REF” and “TEST” with FDR<0.05. Non-directional GO-TermFinder was used to determine GO-enriched processes for differentially expressed genes. GABPA-bound genes were determined from ENCODE GABPA ChIP-seq data for all available cancer cell lines (<http://hgdownload.cse.ucsc.edu/goldenPath/hg19/encodeDCC/wgEncodeRegTfbsClustered/wgEncodeRegTfbsClusteredV3.bed.gz>). BEDOPS closest-features was used to determine transcription start sites within 3 kb of called GABPA peaks presented in 2 samples. These transcription start sites are referred to “GABP-bound genes” throughout the text.

siRNA and LNA-ASO knockdown—Non-targeting, *GABPB1*, and *GABPB2*-directed siRNA pools were obtained from Dharmacon. Scrambled control and *GABPB1L* 3’ UTR-directed Locked Nucleic Acid Antisense Oligonucleotides (LNA-ASOs) were obtained from Exiqon. 100 μ L of cells were seeded at a density of 30,000 cells/mL in a 96-well plate and transfected 24 hr after with a final concentration of 50 nM siRNA or 25 nM LNA-ASO and 0.1 μ L of Dharmafect 1 reagent (Dharmacon). At 48 and 72 hr post-transfection, cells were lysed and cDNA was generated using the POWER SYBR Green Cells-to-Ct kit (Ambion). Quantitative PCR was performed to measure the expression levels of *GUSB*, *TERT*, *GABPB1L*, and *GABPB2* as described below. All siRNAs and LNA-ASOs were independently validated at 48 and 72 hr post-transfection for >50% knockdown of target transcript in all cell lines.

RT-qPCR—Quantitative PCR was performed with POWER SYBR Green Complete Master Mix (Life Technologies) to measure the expression levels of *GUSB* (forward primer: CTCATTTGGAATTTTGCCGATT; reverse primer: CCGAGTGAAGATCCCCTTTTTA), *TERT* (forward primer: TCACGGAGACCACGTTTCAAA; reverse primer: TTCAAGTGCTGTCTGATTCCAAT), *GABPB1* (forward primer: TCCACTTCATCTAGCAGCACA; reverse primer: GTAATGGTGTTCGGTCCACTT), *GABPB1L* (forward primer: ATTGAAAACCGGGTGAATC; reverse primer: CTGTAGGCCTCTGCTTCCTG), *GABPB2* (forward primer: CGCCACCATCGAGATGTCG; reverse primer: TCCAGAGCTATGTCAAAGGCT), *SKP2* (forward primer: ATGCCCAATCTTGTCCATCT; reverse primer: CACCGACTGAGTGATAGGTGT), *COXIV* (forward primer: CAGGGTATTTAGCCTAGTTGGC; reverse primer: GCCGATCCATATAAGCTGGGA), *EIF6* (forward primer: CCGACCAGGTGCTAGTAGGAA; reverse primer: CAGAAGGCACACCAGTCATTC), *TFB1M* (forward primer: GTTGCCACGATTCGAGAAAT; reverse primer: GCCCACTTCGTAAACATAAGCAT), and *RPS16* (forward primer: TCGGACGCAAGAAGACAGC; reverse primer: AGCAGCTTGTACTGTAGCGTG). Each sample was measured in triplicate on the Applied Biosystems 7900HT Fast Real-Time System. Melting curves were manually inspected to confirm PCR specificity. Relative expression levels were calculated by the deltaCT method against *GUSB*.

CRISPR-Cas9 editing—Plasmids encoding spCas9 and sgRNAs were obtained from Addgene (Plasmids #41815 and #47108). Oligonucleotides for construction of sgRNAs were cloned into the sgRNA plasmid as previously described (Brown et al., 2016). Target sequences for sgRNAs are provided in Table S1. Targeting vectors PuroR TV and HygroR TV were acquired and incorporated at target loci as previously described (Gapinske et al., 2018). In brief, LN229, NHAPC5, HEK293T, HCT116, and T98G cells were transfected with Lipofectamine 2000 (Invitrogen) according to the manufacturer's instructions in 24 well plates. GBM1 cells were transfected by electroporation using a Gene Pulser XCell (BioRad) in PBS at 140 Volts, 950 μ F. Each cell line was transfected with equal amounts of Cas9, target sgRNA, targeting vector PuroR TV (GBM1, LN229, HCT116, HEK293T, and T98G) or HygroR TV (NHAPC5) and universal sgRNA. Cleaving of the targeting vector by the universal sgRNA-directed Cas9 allowed for integration of the PuroR or HygroR cassette at the control or *GABPBIL* target loci. Integration only occurs post-cutting of both the targeting vector and target genomic locus. Clonal populations were selected with Puromycin (0.5 μ g/ml HCT116 and T98G, 1 μ g/ml GBM1 and LN229, and 2 μ g/ml HEK293T) or Hygromycin (0.5 μ g/ml for NHAPC5).

Analysis of on-target and off-target editing—Analysis of on-target and off-target mutations was conducted as previously described (Gapinske et al., 2018). In brief, genomic DNA from each clone was isolated using the Animal Genomic DNA Purification Mini Kit (Earthox Life Sciences). PCRs to detect integration of the targeting vector at on-target or off-target sites were performed using KAPA2G Robust PCR kits (Kapa Biosystems) according to the manufacturer's instructions. The DNA sequences of the primers for each target are provided in Table S1. PCR products were visualized in 2% agarose gels and images were captured using a ChemiDoc-It2 (UVP). Indels at off-target sites were analyzed with the Surveyor Mutation Detection kit (IDT) by first amplifying the target locus using PCR with KAPA Robust2G DNA polymerase. The resulting PCR products were melted and reannealed according to manufacturer's instructions, and 18 μ L of the reannealed duplex was mixed with 1 μ L of Surveyor Nuclease and 1 μ L of Enhancer Solution and incubated at 42° Celsius for 1 hr. Final product was loaded onto a 10% TBE polyacrylamide gel and run at 200 V for 30 min. The gels were stained with ethidium bromide and visualized using a ChemiDoc-It2 (UVP). On-target editing of *GABPBIL* (Figure S2A) or control locus (Figure S3B) was evaluated by PCR to detect the integration of the targeting vector. DNA sequencing of the alleles without integration was used to detect indels (Figure S2B). Analysis of off-target mutations was performed by testing integration of the targeting vector at predicted off-target sites (Hsu et al., 2013) in coding regions for each sgRNA used in each cell line (Figures S3A and S3D-F). For predicted off-target sites within coding sequences we performed Surveyor assays to detect indels (Figure S3C).

Immunoblotting—Immunoblotting for Cyclophilin B (loading control) and β 1 (β 1S and β 1L) was performed using a rabbit anti-Cyclophilin B antibody PA1-027A (Pierce antibodies; 1:1,000 dilution) and rabbit anti-GABP β 1 antibody 12597-1-AP (Proteintech; 1:500 dilution) using the NuPAGE system (ThermoFisher), according to the provider's instructions. Detection of primary bands was done using the Li-Cor goat anti-rabbit 680RD secondary antibody (1:15,000 dilution) on the Li-Cor Odyssey Fc imaging system.

NanoBiT protein-protein interaction assay—Full-length *GABPB1L* or *GABPB1S* was cloned into either the pBiT1.1-C [TK/LgBiT] or pBiT2.1-C [TK/LgBiT] vectors (Promega; N196A and N197A, respectively) using In-Fusion HD Cloning (Takara). In accordance with the manufacturer's instructions, the QuikChange Lightning Site-Directed Mutagenesis kit (Agilent) was used to introduce three separate deletions (DEL1-3) into the pBiT1.1-C-GABPB1L vector (see Table S3 for mutagenesis primers). Mutagenized plasmids were validated using Sanger sequencing and purified for use in the NanoBiT assay. Prior to use, 1 volume NanoBiT vector was diluted into 3 volumes of pCMV6-Neo control vector (OriGene) to a final volume of 10 ng/μL. 100 μL of LN229 or NHAPC5 cells were seeded at a density of 30,000 cells/mL in 96-well plates 24 hr prior to transfection. Cells were transfected with a total of 100 ng of plasmid DNA and 0.3 μL X-tremeGENE HP DNA Transfection Reagent (Roche) according to manufacturer's instructions. The following combinations were used to assay β1L tetramer formation in LN229 and NHAPC5 cells:

POS: pBiT1.1-C-GABPB1L-WT + pBiT-2.1-C-GABPB1L

NEG: pBiT1.1-C-GABPB1L-WT + pBiT-2.1-C-GABPB1S

DEL1: pBiT1.1-C-GABPB1L-DEL1 + pBiT-2.1-C-GABPB1L

DEL2: pBiT1.1-C-GABPB1L-DEL2 + pBiT-2.1-C-GABPB1L

DEL3: pBiT1.1-C-GABPB1L-DEL3 + pBiT-2.1-C-GABPB1L

24 hr following transfection, Nano-Glo® Live Cell Substrate diluted in Nano-Glo® LCS Dilution Buffer (Promega; N205A and N206A, respectively) was added directly to the cells and luminescence was assayed 1 hr later on a GloMax® 96 MicroPlate Luminometer (Promega) according to manufacturer's instructions. All data were normalized to the positive control (POS) for each cell line.

Cell proliferation and viability assays—100 μL of cells were seeded at a density of 5,000 cells/mL in 96-well plates. At t=0, 48 and 96 hr post-seeding, MTS (Cell titer 96 aqueous MTS, Promega) was incubated for 2 hr at 37° Celsius in a ratio of 1:5 in media, according to manufacturer's instructions. Plate was read on the Bioplate Synergy 2 microplate reader at 490 nm. Cell proliferation of individual samples was calculated by normalizing absorbance to their corresponding absorbance at t=24 hr. Each time point was analyzed in triplicates. For cell viability, cells were trypsinized, collected and counted on a hemocytometer with trypan-blue exclusion approximately every 7 days from day 33 to day 102 post-editing, or until the minimal sensitivity limits of the assay were reached. Between viability time points, cells were split prior to confluency and replated at 1/8th density to ensure consistent growth conditions. The ratio between viable and dead cells was used to determine cell viability. It is important to note that trypsinization of cells undergoing telomere dysfunction may have influenced to the viability phenotype in the GBM1 and T98G clones after day 85 post-editing.

Chromatin immunoprecipitation—Chromatin immunoprecipitation (ChIP) for GABPa was performed using the ActiveMotif High Sensitivity kit. In brief, GBM1, T98G, HCT116, and HEK293T CRISPR controls and β1L-reduced clones were grown to 80% confluency in 15 cm plates and fixed with 4% formaldehyde. Chromatin was sonicated to a size range of

200–1200 bp by the Diagenode Biorupter. 12–18 μ g of chromatin was used per GABPa (Santa Cruz Biotechnology: sc-22810) and IgG control (Cell Signaling: 2729) immunoprecipitation for each cell type. Enrichment at the *TERT* promoter was determined by qPCR with the ssoAdvanced Universal SYBR Green Supermix (Biorad) supplemented with Resolution Solution from GC-RICH PCR System (Roche). The following primer set was used for qPCR: *TERT+47* (forward: 5'-GCCGGGGCCAGGGCTTCCCA-3'; reverse: 5' CCGCGCTTCCCACGTGGCGG-3'; Tm=74° Celsius). PCR was carried out on the Applied Biosystems 7900HT Fast Real-Time System. Three replicate PCR reactions were carried out for each sample.

Telomere length measurement—All telomere length measurements were conducted using the telomere qPCR protocol initially described in Cawthon 2002 (Cawthon, 2002) and later modified in Lin et al. 2009 (Lin et al., 2010). DNA was collected from CRISPR control and β 1L-reduced cell lines at days 33, 44, 61, 78, and 83 post-CRISPR-Cas9 editing using Phenol:Chloroform:Isoamyl Alcohol (Invitrogen) according to manufacturer's instructions. DNA was diluted to a final concentration of 2 ng/ μ L prior to analysis. Telomere length was measured by qPCR with POWER SYBR Green master mix on the Applied Biosystems 7900HT Fast Real-Time System using the following telomere (TEL) and single gene control (SGC) primer sets: TEL-qPCR, primer forward: CCGTTTGTGGTTTGGGTTTGGGTTTGGGTTTGGGTTTGGGTT, primer reverse: GGCTTGCCCTTACCCTTACCCTTACCCTTACCCTTACCCTTACCCT; SGC-qPCR, primer forward: CAGCAAGTGGGAAGGTGTAATCC primer reverse: CCCATTCTATCATCAACGGGGTACAA (Cawthon, 2002; Lin et al., 2010; Xie et al., 2015). The following PCR conditions were used: 95° Celsius for 10 min followed by 40 cycles of data collection at 95° Celsius for 15 s, 60° Celsius anneal for 30 s and 72° Celsius extend for 30 s along with 80 cycles of melting curve from 60° Celsius to 95° Celsius. Relative telomere length was determined as the linear relationship between TEL and SGC (T/S). Three independent RT-qPCR reactions were carried out for each sample, with each independent experiment performed on distinct days with distinct populations of cells.

Exogenous β 1L and TERT overexpression—*GABPB1L* human cDNA (OriGene) was cloned into pCMV6-Neo Vector (OriGene) using the Cold Fusion Cloning Kit (System Biosciences) according to manufacturer's instructions. The pCMV6-Neo-GABPB1L plasmids obtained were validated by Sanger sequencing using the manufacturer's primers. 2 μ g pCMV6-Neo (empty vector, for control purposes), pCMV6-Neo-B1L or pCI-Neo-hEST2 (Addgene) were transfected into each GBM1, T98G, and LN229 CRISPR control clone (CTRL) or β 1L-reduced clone (C1 and C2) using 6 μ L X-tremeGENE HP DNA Transfection Reagent (Roche) according to producer's instructions at day 61 (GBM1 and T98G) or day 58 (LN229) post-editing. C1/C2 and β 1L/TERT refers to the clone number and cDNA transfected, respectively. Overexpression of exogenous β 1L and TERT mRNA was confirmed by RT-qPCR as described above. Clones were maintained in 100 μ g/mL G418 (Invivogen) and validated for continued *GABPB1L* and *TERT* expression three weeks post-transfection. Lentiviral TERT rescue is described above under the "Orthotopic xenografting and *in vivo* bioluminescent imaging" subheading. pCI neo-hEST2 was a gift from Robert Weinberg (Meyerson et al., 1997) (Addgene plasmid # 1781).

Fluorescent imaging and quantification—CTRL and β 1L-reduced clones were seeded at a density of 25,000 cells/mL on day 70 post-editing. Cells were fixed in 4% formaldehyde and permeabilized in 100% methanol before co-staining with DAPI and anti- γ H2AX AF647 conjugated antibody (EMD Millipore 05-636-AF647) at 4° Celsius overnight. All images were taken at 63 \times magnification on an AxioImager M1 upright fluorescent microscope (Zeiss) with 2.8 ms exposure. Post-processing and signal normalization of images was done using the on-board ZEN2 software. Quantification of extent of chromatin bridge formation and giant cell micronucleation was performed as follows: each slide was assigned a randomized number to blind the quantifier prior to counting. Ten computationally randomized unique 40 \times fields of view with a cell number of $n > 20$ were used per slide. For each field of view, total cell number, number of chromatin bridges, and number of giant micronucleated cells were counted. Only nuclei completely in the field of view were counted. A chromatin bridge was defined as a solid strand of nuclear material linking two distinctly independent nuclei. Two nuclei linked by a chromatin bridge were counted as one cell. A giant micronucleated cell was defined as a single cell containing $n \geq 5$ uncondensed nuclei. The weighted proportion of chromatin bridges and giant micronucleated cells was determined per field of view and summed into an aggregate proportion. All methods and quantifications were verified using the same parameters as described above by an independent party. Quantification of γ H2AX was performed similarly to chromatin bridge and giant cell micronucleation counting with the following differences: $n > 10$ cells per field of view was used as a threshold and individual visible γ H2AX foci were counted per cell per field of view. This procedure was likewise followed to quantify LN229 clones at day 45 and day 61 post-editing ($n = 4$ fields of view).

Flow cytometry—On day 75 post-editing, 300,000 cells/line were stained with a combination of Hoechst® 33342 (Thermofisher; 10 ng/mL), AnnexinV-PE (BD Biosciences #51-65875X; 1:1,000 dilution), and C-12-FDG (Setareh Biotech; 33 μ M final concentration) for 45 min at 37° Celsius in the dark. Samples were run for 10,000 counts on a Sony SH800 cytometer and analyzed on FlowJo®. The same gating strategy was used for all experiments. All data were collected ONLY after a stable flow of cells had been established. Then, FSC-A vs. FSC-H gating was used to select for singlets along the positive diagonal. Next, FSC-A vs. SSC-A gating was used to remove all cellular debris (FSC-A/SSC-A low particles). Finally, non-specific antibody/fluorophore uptake was used to gate against dead cells with compromised membranes.

Quantification and statistical analysis

All statistical analysis was done using GraphPad Prism 7. Non-parametric Spearman correlation was used for GABP isoforms versus *TERT* and telomere length versus viability analysis ($\alpha = 0.05$). Adjusted p values after multiple comparison correction are reported for each correlation. A non-parametric Spearman correlation was chosen due to the failure of a subset of data sets to meet the homoscedasticity assumption of the Pearson test. Mouse survival data for the orthotopic xenograft experiments were analyzed with the Kaplan-Meier Log-Rank Test ($\alpha = 0.05$). The non-parametric Welch's t-test was used as listed for samples with unequal sample sizes ($\alpha = 0.05$). A two-sided heteroscedastic Student's t-test was used as listed for all other assays ($\alpha = 0.05$) after confirming differences in variances between

tested groups. All error bars shown are mean \pm S.D. A sample size of 3 independent experiments (biological replicates) was used for all experiments, unless otherwise noted, in order to ensure appropriate statistical power to detect a statistically significant change of at least two-fold. 3 technical replicates per biological replicate were used for each experiment as noted.

Data and software availability

All data used for GABP isoform and *TERT* expression correlations are available for public access from the TCGA (level 3 normalized data, December 2015, <http://tcga-data.nci.nih.gov/tcga/dataAccessMatrix.htm>). All raw data used for RNA-seq analysis has been deposited in the European Genome Archive (EGA) under ID code EGAS0000100258.2. Scripts used for RNA-seq analysis are available at <https://github.com/UCSF-Costello-Lab/Tert-gabp>.

Supplementary Material

Refer to Web version on PubMed Central for supplementary material.

Acknowledgements:

This work was supported by a generous gift from the Dabbiere family (J.F.C.), the Hana Jabsheh Research Initiative (J.F.C.), NIH grants NCI P50CA097257 (J.F.C. and J.A.D.), NCI P01CA118816-06 (J.F.C.), T32 GM008568 and T32 CA151022 (A.M.), and NCI R01CA163336 (J.S.S.), and the Sontag Foundation Distinguished Scientist Award (J.S.S.). C.F. is supported by a US National Institutes of Health K99/R00 Pathway to Independence Award (K99GM118909) from the National Institute of General Medical Sciences (NIGMS). Additional support was provided by Fundação para a Ciência e Tecnologia SFRH/BD/88220/2012 (A.X.-M.) and IF/00601/2012 (B.M.C.). J.A.D. is an investigator of the Howard Hughes Medical Institute.

References:

- Akincilar S, Khattar E, Boon PL, Unal B, Fullwood MJ, and Tergaonkar V (2016). Long-range chromatin interactions drive mutant Tert promoter activation. *Cancer Discov*.
- Arita H, Narita Y, Fukushima S, Tateishi K, Matsushita Y, Yoshida A, Miyakita Y, Ohno M, Collins VP, Kawahara N, et al. (2013). Upregulating mutations in the TERT promoter commonly occur in adult malignant gliomas and are strongly associated with total 1p19q loss. *Acta neuropathologica* 126, 267–276. [PubMed: 23764841]
- Barszczyk M, Buczkowicz P, Castelo-Branco P, Mack SC, Ramaswamy V, Mangerel J, Agnihotri S, Remke M, Golbourn B, Pajovic S, et al. (2014). Telomerase inhibition abolishes the tumorigenicity of pediatric ependymoma tumor-initiating cells. *Acta neuropathologica* 128, 863–877. [PubMed: 25120190]
- Bell RJ, Rube HT, Kreig A, Mancini A, Fouse SD, Nagarajan RP, Choi S, Hong C, He D, Pekmezci M, et al. (2015). Cancer. The transcription factor GABP selectively binds and activates the mutant TERT promoter in cancer. *Science* 348, 1036–1039. [PubMed: 25977370]
- Bell RJ, Rube HT, Xavier-Magalhaes A, Costa BM, Mancini A, Song JS, and Costello JF (2016). Understanding TERT Promoter Mutations: A Common Path to Immortality. *Molecular cancer research : MCR* 14, 315–323. [PubMed: 26941407]
- Blackburn EH, Greider CW, and Szostak JW (2006). Telomeres and telomerase: the path from maize, Tetrahymena and yeast to human cancer and aging. *Nat Med* 12, 1133–1138. [PubMed: 17024208]
- Brown A, Woods WS, and Perez-Pinera P (2016). Multiplexed Targeted Genome Engineering Using a Universal Nuclease-Assisted Vector Integration System. *ACS Synth Biol* 5, 582–588. [PubMed: 27159246]

- Bryan TM, and Cech TR (1999). Telomerase and the maintenance of chromosome ends. *Current opinion in cell biology* 11, 318–324. [PubMed: 10395557]
- Cancer Genome Atlas Research, N. (2008). Comprehensive genomic characterization defines human glioblastoma genes and core pathways. *Nature* 455, 1061–1068. [PubMed: 18772890]
- Cao Y, Li H, Deb S, and Liu JP (2002). TERT regulates cell survival independent of telomerase enzymatic activity. *Oncogene* 21, 3130–3138. [PubMed: 12082628]
- Capper R, Britt-Compton B, Tankimanova M, Rowson J, Letsolo B, Man S, Haughton M, and Baird DM (2007). The nature of telomere fusion and a definition of the critical telomere length in human cells. *Genes & development* 21, 2495–2508. [PubMed: 17908935]
- Carter RS, and Avadhani NG (1994). Cooperative binding of GA-binding protein transcription factors to duplicated transcription initiation region repeats of the cytochrome c oxidase subunit IV gene. *J Biol Chem* 269, 4381–4387. [PubMed: 8308008]
- Castelo-Branco P, Zhang C, Lipman T, Fujitani M, Hansford L, Clarke I, Harley CB, Tressler R, Malkin D, Walker E, et al. (2011). Neural tumor-initiating cells have distinct telomere maintenance and can be safely targeted for telomerase inhibition. *Clinical cancer research : an official journal of the American Association for Cancer Research* 17, 111–121. [PubMed: 21208905]
- Cawthon RM (2002). Telomere measurement by quantitative PCR. *Nucleic acids research* 30, e47. [PubMed: 12000852]
- Ceccarelli M, Barthel FP, Malta TM, Sabedot TS, Salama SR, Murray BA, Morozova O, Newton Y, Radenbaugh A, Pagnotta SM, et al. (2016). Molecular Profiling Reveals Biologically Discrete Subsets and Pathways of Progression in Diffuse Glioma. *Cell* 164, 550–563. [PubMed: 26824661]
- Chaires JB, Trent JO, Gray RD, Dean WL, Buscaglia R, Thomas SD, and Miller DM (2014). An improved model for the hTERT promoter quadruplex. *PLoS One* 9, e115580. [PubMed: 25526084]
- Chiba K, Johnson JZ, Vogan JM, Wagner T, Boyle JM, and Hockemeyer D (2015). Cancer-associated TERT promoter mutations abrogate telomerase silencing. *Elife* 4.
- Chiba K, Lorbeer FK, Shain AH, McSwiggen DT, Schruf E, Oh A, Ryu J, Darzacq X, Bastian BC, and Hockemeyer D (2017). Mutations in the promoter of the telomerase gene TERT contribute to tumorigenesis by a two-step mechanism. *Science* 357, 1416–1420. [PubMed: 28818973]
- Chin L, Artandi SE, Shen Q, Tam A, Lee SL, Gottlieb GJ, Greider CW, and DePinho RA (1999). p53 deficiency rescues the adverse effects of telomere loss and cooperates with telomere dysfunction to accelerate carcinogenesis. *Cell* 97, 527–538. [PubMed: 10338216]
- Chinenov Y, Henzl M, and Martin ME (2000). The alpha and beta subunits of the GA-binding protein form a stable heterodimer in solution. Revised model of heterotetrameric complex assembly. *The Journal of biological chemistry* 275, 7749–7756. [PubMed: 10713087]
- Counter CM, Avilion AA, LeFeuvre CE, Stewart NG, Greider CW, Harley CB, and Bacchetti S (1992). Telomere shortening associated with chromosome instability is arrested in immortal cells which express telomerase activity. *The EMBO journal* 11, 1921–1929. [PubMed: 1582420]
- Counter CM, Meyerson M, Eaton EN, Ellisen LW, Caddle SD, Haber DA, and Weinberg RA (1998). Telomerase activity is restored in human cells by ectopic expression of hTERT (hEST2), the catalytic subunit of telomerase. *Oncogene* 16, 1217–1222. [PubMed: 9528864]
- de la Brousse FC, Birkenmeier EH, King DS, Rowe LB, and McKnight SL (1994). Molecular and genetic characterization of GABP beta. *Genes & development* 8, 1853–1865. [PubMed: 7958862]
- Deeraksa A, Pan J, Sha Y, Liu XD, Eissa NT, Lin SH, and Yu-Lee LY (2013). Plk1 is upregulated in androgen-insensitive prostate cancer cells and its inhibition leads to necroptosis. *Oncogene* 32, 2973–2983. [PubMed: 22890325]
- der-Sarkissian H, Bacchetti S, Cazes L, and Londono-Vallejo JA (2004). The shortest telomeres drive karyotype evolution in transformed cells. *Oncogene* 23, 1221–1228. [PubMed: 14716292]
- Donadini A, Giacomelli F, Ravazzolo R, Gandin V, Marchisio PC, and Biffo S (2006). GABP complex regulates transcription of eIF6 (p27BBP), an essential trans-acting factor in ribosome biogenesis. *FEBS Lett* 580, 1983–1987. [PubMed: 16530192]
- Fitzgerald MS, Riha K, Gao F, Ren S, McKnight TD, and Shippen DE (1999). Disruption of the telomerase catalytic subunit gene from Arabidopsis inactivates telomerase and leads to a slow loss

- of telomeric DNA. *Proceedings of the National Academy of Sciences of the United States of America* 96, 14813–14818. [PubMed: 10611295]
- Fouse SD, Nakamura JL, James CD, Chang S, and Costello JF (2014). Response of primary glioblastoma cells to therapy is patient specific and independent of cancer stem cell phenotype. *Neuro-oncology* 16, 361–371. [PubMed: 24311636]
- Fragkos M, and Beard P (2011). Mitotic catastrophe occurs in the absence of apoptosis in p53-null cells with a defective G1 checkpoint. *PLoS One* 6, e22946. [PubMed: 21853057]
- Gapinske M, Tague N, Winter J, Underhill GH, and Perez-Pinera P (2018). Targeted Gene Knock Out Using Nuclease-Assisted Vector Integration: Hemi- and Homozygous Deletion of JAG1. *Methods Mol Biol* 1772, 233–248. [PubMed: 29754232]
- Genuario RR, and Perry RP (1996). The GA-binding protein can serve as both an activator and repressor of ribosomal protein gene transcription. *J Biol Chem* 271, 4388–4395. [PubMed: 8626789]
- Hackett JA, Feldser DM, and Greider CW (2001). Telomere dysfunction increases mutation rate and genomic instability. *Cell* 106, 275–286. [PubMed: 11509177]
- Hayashi MT, Cesare AJ, Rivera T, and Karlseder J (2015). Cell death during crisis is mediated by mitotic telomere deprotection. *Nature* 522, 492–496. [PubMed: 26108857]
- Horn S, Figl A, Rachakonda PS, Fischer C, Sucker A, Gast A, Kadel S, Moll I, Nagore E, Hemminki K, et al. (2013). TERT promoter mutations in familial and sporadic melanoma. *Science* 339, 959–961. [PubMed: 23348503]
- Hsu PD, Scott DA, Weinstein JA, Ran FA, Konermann S, Agarwala V, Li Y, Fine EJ, Wu X, Shalem O, et al. (2013). DNA targeting specificity of RNA-guided Cas9 nucleases. *Nat Biotechnol* 31, 827–832. [PubMed: 23873081]
- Huang FW, Hodis E, Xu MJ, Kryukov GV, Chin L, and Garraway LA (2013). Highly recurrent TERT promoter mutations in human melanoma. *Science* 339, 957–959. [PubMed: 23348506]
- Ianzini F, and Mackey MA (1997). Spontaneous premature chromosome condensation and mitotic catastrophe following irradiation of HeLa S3 cells. *Int J Radiat Biol* 72, 409–421. [PubMed: 9343106]
- Iwado E, Daido S, Kondo Y, and Kondo S (2007). Combined effect of 2–5A-linked antisense against telomerase RNA and conventional therapies on human malignant glioma cells in vitro and in vivo. *International journal of oncology* 31, 1087–1095. [PubMed: 17912434]
- Jager K, and Walter M (2016). Therapeutic Targeting of Telomerase. *Genes* 7.
- Jing X, Zhao DM, Waldschmidt TJ, and Xue HH (2008). GABPbeta2 is dispensible for normal lymphocyte development but moderately affects B cell responses. *J Biol Chem* 283, 24326–24333. [PubMed: 18628204]
- Killela PJ, Reitman ZJ, Jiao Y, Bettegowda C, Agrawal N, Diaz LA, Jr., Friedman AH, Friedman H, Gallia GL, Giovanella BC, et al. (2013). TERT promoter mutations occur frequently in gliomas and a subset of tumors derived from cells with low rates of self-renewal. *Proceedings of the National Academy of Sciences of the United States of America* 110, 6021–6026. [PubMed: 23530248]
- Kim NW, Piatyszek MA, Prowse KR, Harley CB, West MD, Ho PL, Coviello GM, Wright WE, Weinrich SL, and Shay JW (1994). Specific association of human telomerase activity with immortal cells and cancer. *Science* 266, 2011–2015. [PubMed: 7605428]
- Li Y, Zhou QL, Sun W, Chandrasekharan P, Cheng HS, Ying Z, Lakshmanan M, Raju A, Tenen DG, Cheng SY, et al. (2015). Non-canonical NF-kappaB signalling and ETS1/2 cooperatively drive C250T mutant TERT promoter activation. *Nat Cell Biol* 17, 1327–1338. [PubMed: 26389665]
- Lim KW, Lacroix L, Yue DJ, Lim JK, Lim JM, and Phan AT (2010). Coexistence of two distinct G-quadruplex conformations in the hTERT promoter. *J Am Chem Soc* 132, 12331–12342. [PubMed: 20704263]
- Lin J, Epel E, Cheon J, Kroenke C, Sinclair E, Bigos M, Wolkowitz O, Mellon S, and Blackburn E (2010). Analyses and comparisons of telomerase activity and telomere length in human T and B cells: insights for epidemiology of telomere maintenance. *J Immunol Methods* 352, 71–80. [PubMed: 19837074]

- Makowski MM, Willems E, Fang J, Choi J, Zhang T, Jansen PW, Brown KM, and Vermeulen M (2016). An interaction proteomics survey of transcription factor binding at recurrent TERT promoter mutations. *Proteomics* 16, 417–426. [PubMed: 26553150]
- Marian CO, Cho SK, McEllin BM, Maher EA, Hatanpaa KJ, Madden CJ, Mickey BE, Wright WE, Shay JW, and Bachoo RM (2010). The telomerase antagonist, imetelstat, efficiently targets glioblastoma tumor-initiating cells leading to decreased proliferation and tumor growth. *Clinical cancer research : an official journal of the American Association for Cancer Research* 16, 154–163.
- Meyerson M, Counter CM, Eaton EN, Ellisen LW, Steiner P, Caddle SD, Ziaugra L, Beijersbergen RL, Davidoff MJ, Liu Q, et al. (1997). hEST2, the putative human telomerase catalytic subunit gene, is up-regulated in tumor cells and during immortalization. *Cell* 90, 785–795. [PubMed: 9288757]
- Ohba S, Mukherjee J, Johannessen TC, Mancini A, Chow TT, Wood M, Jones L, Mazor T, Marshall RE, Viswanath P, et al. (2016). Mutant IDH1 Expression Drives TERT Promoter Reactivation as Part of the Cellular Transformation Process. *Cancer Res* 76, 6680–6689. [PubMed: 27758882]
- Reyes-Uribe P, Adrianzen-Ruesta MP, Deng Z, Echevarria-Vargas I, Mender I, Saheb S, Liu Q, Altieri DC, Murphy ME, Shay JW, et al. (2018). Exploiting TERT dependency as a therapeutic strategy for NRAS-mutant melanoma. *Oncogene*.
- Rosmarin AG, Resendes KK, Yang Z, McMillan JN, and Fleming SL (2004). GA-binding protein transcription factor: a review of GABP as an integrator of intracellular signaling and protein-protein interactions. *Blood Cells Mol Dis* 32, 143–154. [PubMed: 14757430]
- Saretzki G, Sitte N, Merkel U, Wurm RE, and von Zglinicki T (1999). Telomere shortening triggers a p53-dependent cell cycle arrest via accumulation of G-rich single stranded DNA fragments. *Oncogene* 18, 5148–5158. [PubMed: 10498864]
- Sawada J, Goto M, Sawa C, Watanabe H, and Handa H (1994). Transcriptional activation through the tetrameric complex formation of E4TF1 subunits. *EMBO J* 13, 1396–1402. [PubMed: 8137823]
- Shay JW, and Wright WE (2000). Hayflick, his limit, and cellular ageing. *Nat Rev Mol Cell Biol* 1, 72–76. [PubMed: 11413492]
- Shay JW, and Wright WE (2006). Telomerase therapeutics for cancer: challenges and new directions. *Nat Rev Drug Discov* 5, 577–584. [PubMed: 16773071]
- Spiegel-Kreinecker S, Lotsch D, Ghanim B, Pirker C, Mohr T, Laaber M, Weis S, Olschowski A, Webersinke G, Pichler J, and Berger W (2015). Prognostic quality of activating TERT promoter mutations in glioblastoma: interaction with the rs2853669 polymorphism and patient age at diagnosis. *Neuro-oncology* 17, 1231–1240. [PubMed: 25681309]
- Stern JL, Theodorescu D, Vogelstein B, Papadopoulos N, and Cech TR (2015). Mutation of the TERT promoter, switch to active chromatin, and monoallelic TERT expression in multiple cancers. *Genes & development* 29, 2219–2224. [PubMed: 26515115]
- Vakifahmetoglu H, Olsson M, and Zhivotovsky B (2008). Death through a tragedy: mitotic catastrophe. *Cell Death Differ* 15, 1153–1162. [PubMed: 18404154]
- Vinagre J, Almeida A, Populo H, Batista R, Lyra J, Pinto V, Coelho R, Celestino R, Prazeres H, Lima L, et al. (2013). Frequency of TERT promoter mutations in human cancers. *Nat Commun* 4, 2185. [PubMed: 23887589]
- Vitale I, Galluzzi L, Castedo M, and Kroemer G (2011). Mitotic catastrophe: a mechanism for avoiding genomic instability. *Nat Rev Mol Cell Biol* 12, 385–392. [PubMed: 21527953]
- Wang F, Pan X, Kalmbach K, Seth-Smith ML, Ye X, Antunes DM, Yin Y, Liu L, Keefe DL, and Weissman SM (2013). Robust measurement of telomere length in single cells. *Proceedings of the National Academy of Sciences of the United States of America* 110, E1906–1912. [PubMed: 23661059]
- Whitaker NJ, Bryan TM, Bonnefin P, Chang AC, Musgrove EA, Braithwaite AW, and Reddel RR (1995). Involvement of RB-1, p53, p16INK4 and telomerase in immortalisation of human cells. *Oncogene* 11, 971–976. [PubMed: 7675456]
- Xie Z, Jay KA, Smith DL, Zhang Y, Liu Z, Zheng J, Tian R, Li H, and Blackburn EH (2015). Early telomerase inactivation accelerates aging independently of telomere length. *Cell* 160, 928–939. [PubMed: 25723167]

- Xu M, Lee EM, Wen Z, Cheng Y, Huang WK, Qian X, Tcw J, Kouznetsova J, Ogden SC, Hammack C, et al. (2016). Identification of small-molecule inhibitors of Zika virus infection and induced neural cell death via a drug repurposing screen. *Nat Med* 22, 1101–1107. [PubMed: 27571349]
- Xue HH, Jing X, Bollenbacher-Reilley J, Zhao DM, Haring JS, Yang B, Liu C, Bishop GA, Harty JT, and Leonard WJ (2008). Targeting the GA binding protein beta1L isoform does not perturb lymphocyte development and function. *Mol Cell Biol* 28, 4300–4309. [PubMed: 18426908]
- Yang ZF, Drumea K, Mott S, Wang J, and Rosmarin AG (2014). GABP transcription factor (nuclear respiratory factor 2) is required for mitochondrial biogenesis. *Mol Cell Biol* 34, 3194–3201. [PubMed: 24958105]
- Yang ZF, Mott S, and Rosmarin AG (2007). The Ets transcription factor GABP is required for cell-cycle progression. *Nature cell biology* 9, 339–346. [PubMed: 17277770]
- Yu M, Yang XY, Schmidt T, Chinenov Y, Wang R, and Martin ME (1997). GA-binding protein-dependent transcription initiator elements. Effect of helical spacing between polyomavirus enhancer a factor 3(PEA3)/Ets-binding sites on initiator activity. *J Biol Chem* 272, 29060–29067. [PubMed: 9360980]
- Yu S, Jing X, Colgan JD, Zhao DM, and Xue HH (2012). Targeting tetramer-forming GABPbeta isoforms impairs self-renewal of hematopoietic and leukemic stem cells. *Cell Stem Cell* 11, 207–219. [PubMed: 22862946]
- Zehir A, Benayed R, Shah RH, Syed A, Middha S, Kim HR, Srinivasan P, Gao J, Chakravarty D, Devlin SM, et al. (2017). Mutational landscape of metastatic cancer revealed from prospective clinical sequencing of 10,000 patients. *Nat Med* 23, 703–713. [PubMed: 28481359]

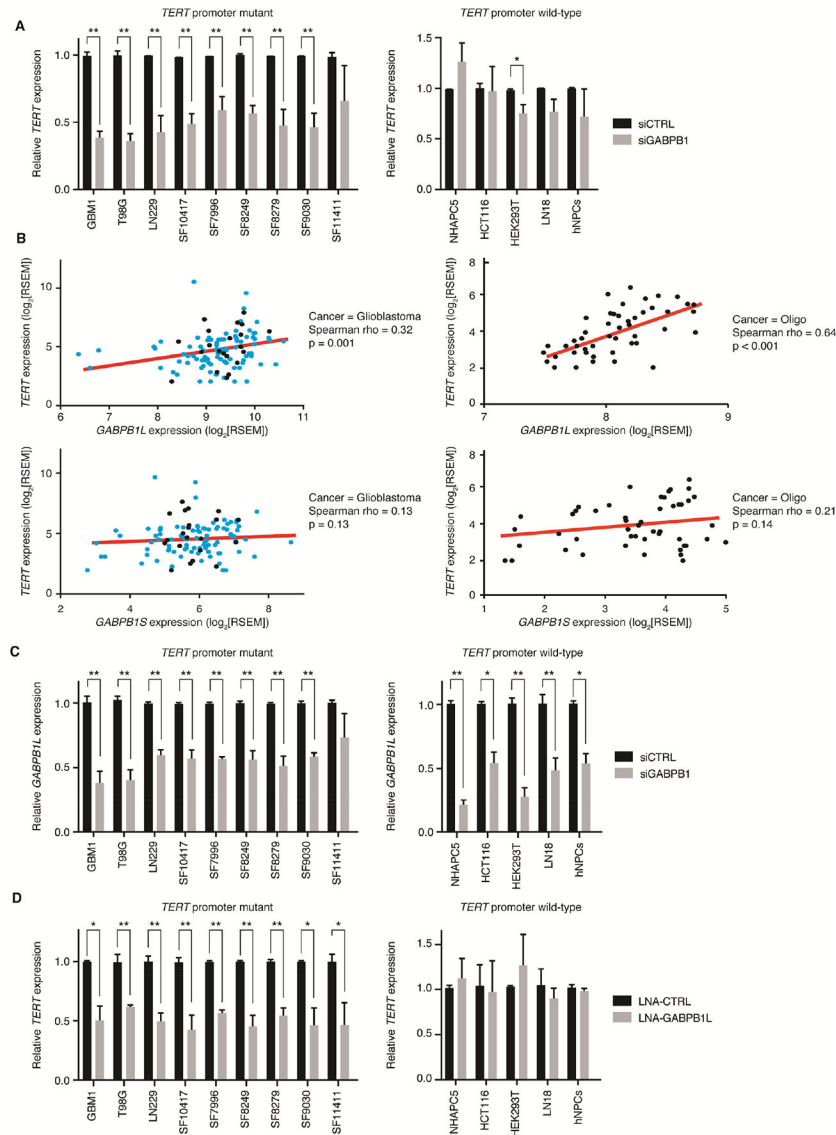
Significance

TERT promoter mutations are the third most common mutation in human cancer, and the single most common mutation in glioblastoma. Understanding how the promoter mutation leads to tumor cell immortality could uncover potential targets to undermine immortality and reduce tumor growth. *TERT* promoter mutations selectively recruit the transcription factor GABP to activate *TERT* expression across multiple types of cancer. Our results suggest that the normally dispensable β 1L isoform of GABP is a key to tumor cell immortality in *TERT* promoter mutant brain tumors. Inhibiting GABP β 1L may be an approach to reverse tumor cell immortality while sparing *TERT* promoter wild-type cells.

Highlights

- The β 1L tetramer-forming isoform of GABP activates the mutant *TERT* promoter
- β 1L disruption induces telomere loss and death only in *TERT* promoter mutant cells
- Disruption of β 1L reduces tumor growth and prolongs survival in xenografted mice
- GABP β 1L is a potential therapeutic target for *TERT* promoter mutant glioblastoma

TERT promoter mutations generate a binding site for GABP and reactivate *TERT* expression. Mancini et al. show that GABP β 1L, among GABP subunits, is specifically required for the function of *TERT* promoter mutants, reducing GABP β 1L causes telomere loss and cell death exclusively in *TERT* promoter mutant cells.

**Figure 1.**

The GABP tetramer-forming isoform $\beta 1L$ positively regulates *TERT* expression solely in *TERT* promoter mutant tumor cells. (A) *TERT* expression following siRNA-mediated knockdown of $\beta 1$ (siGABPB1) in *TERT* promoter mutant (left) or *TERT* promoter-wild-type (right) cell lines and primary cultures. *p value < 0.05, **p value < 0.01, two-sided Student's t-test compared to a non-targeting siRNA control (siCTRL) in each respective line. (B) Correlation of *GABPB1L* (top graphs) or *GABPB1S* (bottom graphs) expression (log₂[RSEM normalized counts]) versus *TERT* expression (log₂[RSEM normalized counts]) from 109 *TERT*-expressing GBMs (left graphs) or 49 *TERT* promoter-mutant oligodendrogliomas (right graphs). Red line indicates trend line. Black points indicate Sanger-validated *TERT* promoter mutant GBM and oligodendroglioma samples, teal points are GBM samples that were not tested for *TERT* promoter mutation status. Spearman's Rank-Order Correlation was used to generate Spearman rho and p values for each

correlation. **(C)** *GABPB1L* expression following siRNA-mediated knockdown of $\beta 1$ (siGABPB1) in *TERT* promoter mutant (left) and wild-type (right) lines. *p value<0.05, **p value<0.01, two-sided Student's t-test compared to a non-targeting siRNA control (siCTRL) in each respective line. **(D)** *TERT* expression following LNA-ASO knockdown of $\beta 1L$ (LNA-GABPB1L) in *TERT* promoter mutant (left) or wild-type (right) cell lines and primary cultures compared to a control LNA-ASO (LNA-CTRL). *p value<0.05, **p value<0.01, two-sided Student's t-test compared to LNA-CTRL in each respective line. Values are mean \pm S.D. of at least three independent experiments (A, C, and D; two independent experiments for SF10417). See also Figure S1.

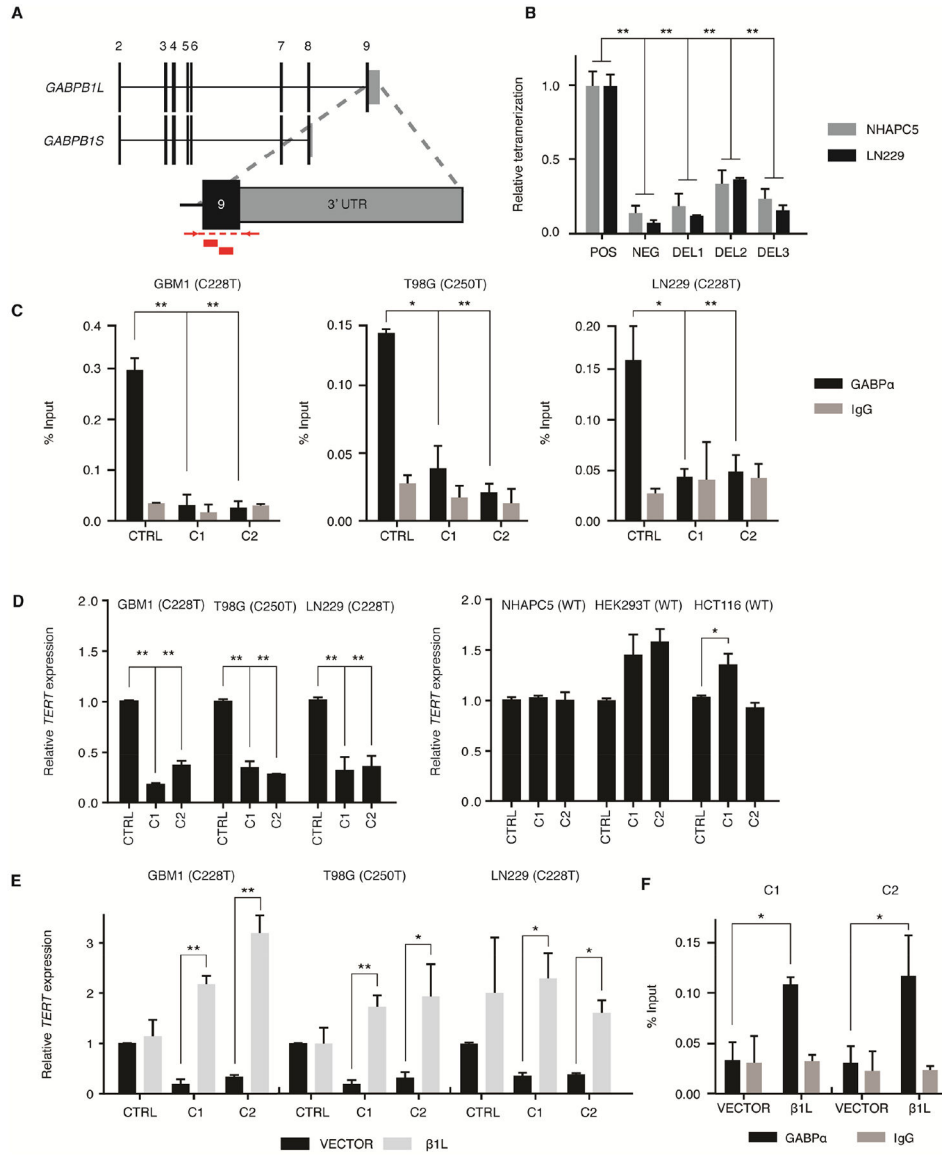


Figure 2. CRISPR-Cas9-mediated disruption of *GABPB1L* reduces GABP-mediated activation of the mutant *TERT* promoter. (A) Exon structure for the *GABPB1* locus, depicting the *GABPB1S* and *GABPB1L* isoforms. Inset shows targeting strategy for CRISPR-Cas9 editing of *GABPB1L*. Red blocks indicate sgRNA target sites. Red arrows and dashed lines indicate primer locations and target amplicon for PCR validation of editing. (B) Quantification of β 1L tetramerization in the wild-type (POS) or mutated (DEL1-3) state. The negative (NEG) state consists of one β 1L vector and one β 1S vector, the products of which are unable to form a tetramer. *p value<0.05, **p value<0.01, two-sided Student's t-test of DEL1-3 or NEG respective to the positive control (POS). (C) GABP α or IgG control ChIP-qPCR for the *TERT* promoter in CRISPR control (CTRL) or β 1L-reduced clones (C1 and C2). *p value<0.05, **p value<0.01, two-sided Student's t-test compared to respective CTRL. (D) *TERT* expression relative to CTRL for β 1L-reduced *TERT* promoter mutant (left) or wild-

type (right) clones. *p value<0.05, **p value<0.01, two-sided Student's t-test compared to CTRL. (E,F) *TERT* expression (E) or GABP α occupancy (F) in β 1L-reduced clones relative to CTRL 48 hr following transfection with empty (VECTOR) or β 1L expression vector. *p value<0.05, **p value<0.01, two-sided Student's t-test compared to respective VECTOR control. Values are mean \pm S.D. of at least two independent experiments (C and F) or three independent experiments (B, D, and E). See also Figures S2–S3 and Tables S1–S3.

Author Manuscript

Author Manuscript

Author Manuscript

Author Manuscript

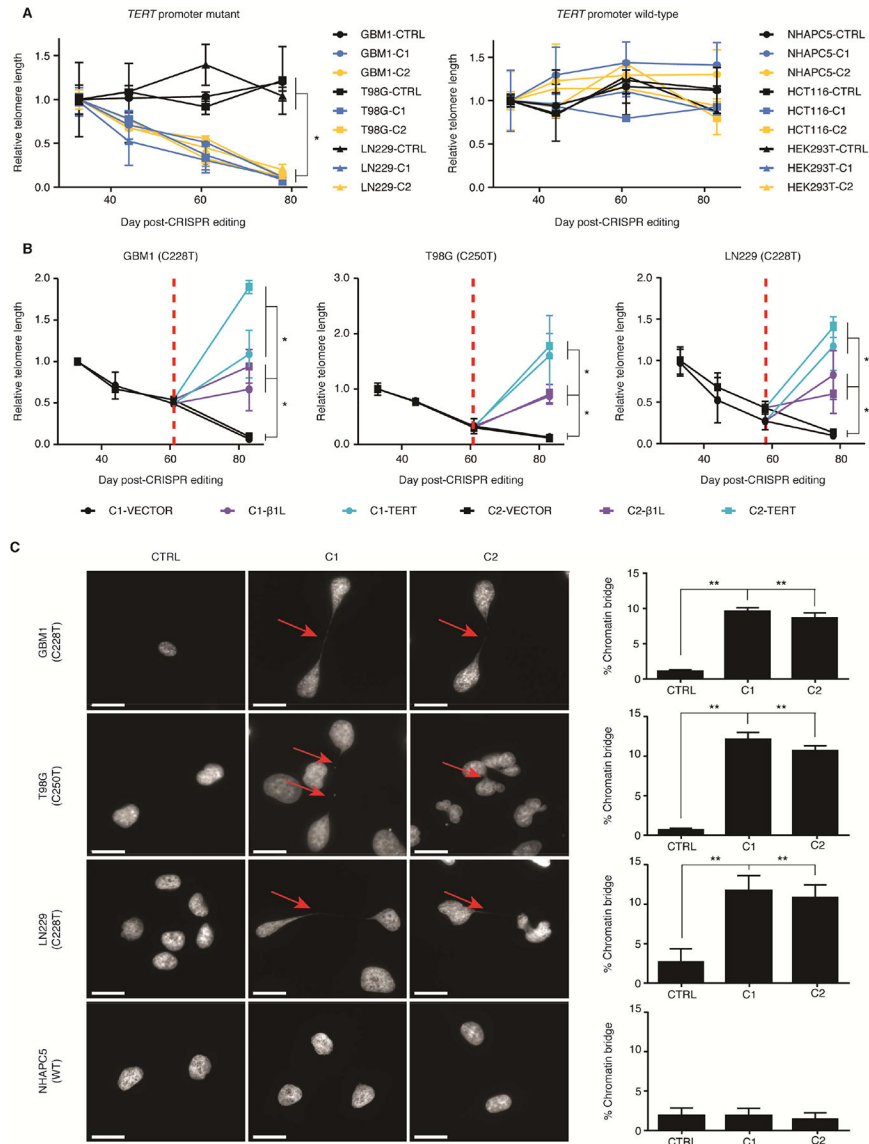


Figure 3. β 1L-mediated activation of the mutant *TERT* promoter is required for telomere maintenance in GBM. **(A)** Telomere length at days 44, 61, and 78 in *TERT* promoter mutant lines or days 44, 61 and 83 in *TERT* promoter wild-type lines post-editing relative to day 33 post-editing for CTRL or β 1L-reduced clones. *p value<0.05, two-sided Student’s t-test comparing values between CTRL and β 1L-reduced clones at day 78/83 for each respective line. Values are mean \pm S.D. of at least three independent assays. **(B)** Relative telomere length after transfection of an empty (VECTOR), β 1L, or TERT expression vector in *TERT* promoter-mutant lines 78 or 83 days post-editing. Red dotted line indicates time of transfection (at day 58 [LN229] or 61 [GBM1 and T98G] post-editing). *p value<0.05, two-sided Student’s t-test of values of β 1L or TERT versus VECTOR at day 78/83. Values are mean \pm S.D. of at least three independent experiments. **(C)** Representative DAPI images (left images) and quantification (right graphs) of chromatin bridges (arrow) in CTRL or β 1L-reduced clones at

days 70–75 post-editing. Scale bar = 20 μm . *p value<0.05, **p value<0.01, two-sided Student's t-test compared to CTRL. Quantification values are weighted mean \pm S.D. of at least ten independent fields of view. See also Figure S4.

Author Manuscript

Author Manuscript

Author Manuscript

Author Manuscript

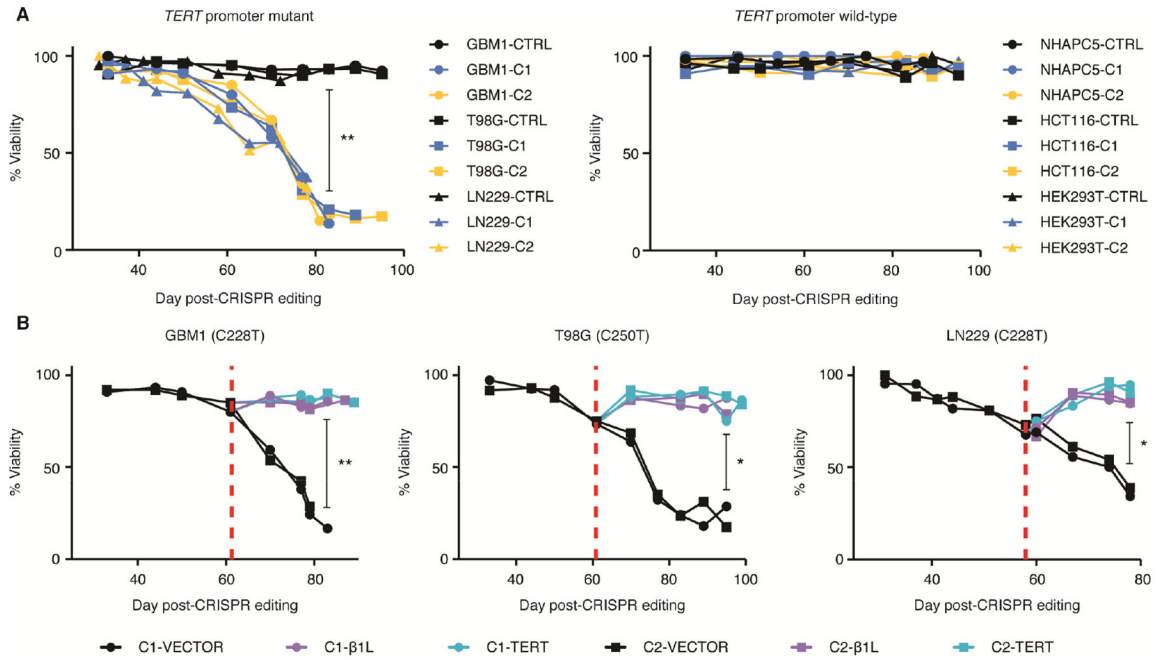
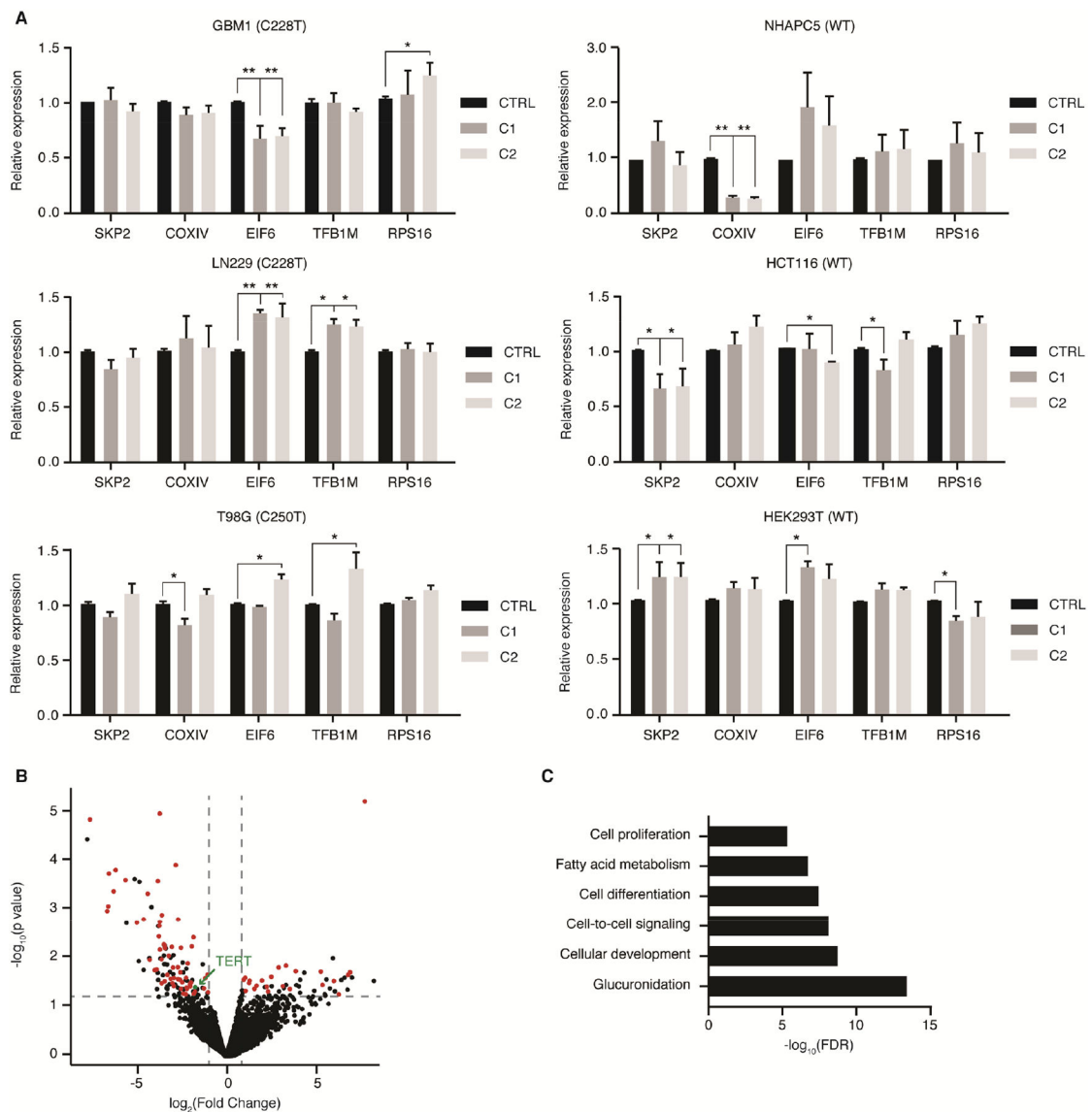


Figure 4. β 1L reduction induces loss of replicative immortality in *TERT* promoter-mutant GBM lines. (A) Cell viability of CTRL or β 1L-reduced clones measured approximately every 7 days from day 33 to day 99 post-editing for *TERT* promoter mutant and wild-type lines. **p value<0.01, Welch’s t-test of CTRL clones versus β 1L-reduced clones at day 83 post-editing. (B) Cell viability measurements following transfection with an empty (VECTOR), β 1L, or TERT expression vector. Red dotted line indicates time of transfection. *p value<0.05, **p value<0.01, Welch’s t-test of vector transfected cells versus β 1L and TERT transfected cells at the final recorded time-point for each line. Values are median of three independent experiments. See also Figure S5.

**Figure 5.**

β 1L regulates a subset of GABP transcription factor targets in GBM cells. **(A)** Expression of one GABP dimer target and four GABP tetramer targets relative to CTRL for β 1L-reduced clones derived from *TERT* promoter mutant and wild-type lines at day 45 post-editing. *p value < 0.05, **p value < 0.01, two-sided Student's t-test compared to CTRL. Values are mean \pm S.D of at least three independent assays. **(B)** Volcano plot of expression differences between CTRL and β 1L-reduced *TERT* promoter mutant lines (GBM1, T98G, and LN229) as determined via RNA-seq at day 45 post-editing. Maroon-colored points represent putative GABP-regulated genes that are differentially expressed (\log_2 Fold Change > 1 & FDR < 0.05). **(C)** GO-terms analysis of 161 genes that are commonly differentially expressed genes between CTRL and multiple β 1L-reduced *TERT* promoter mutant lines. See also Tables S4 and S5.

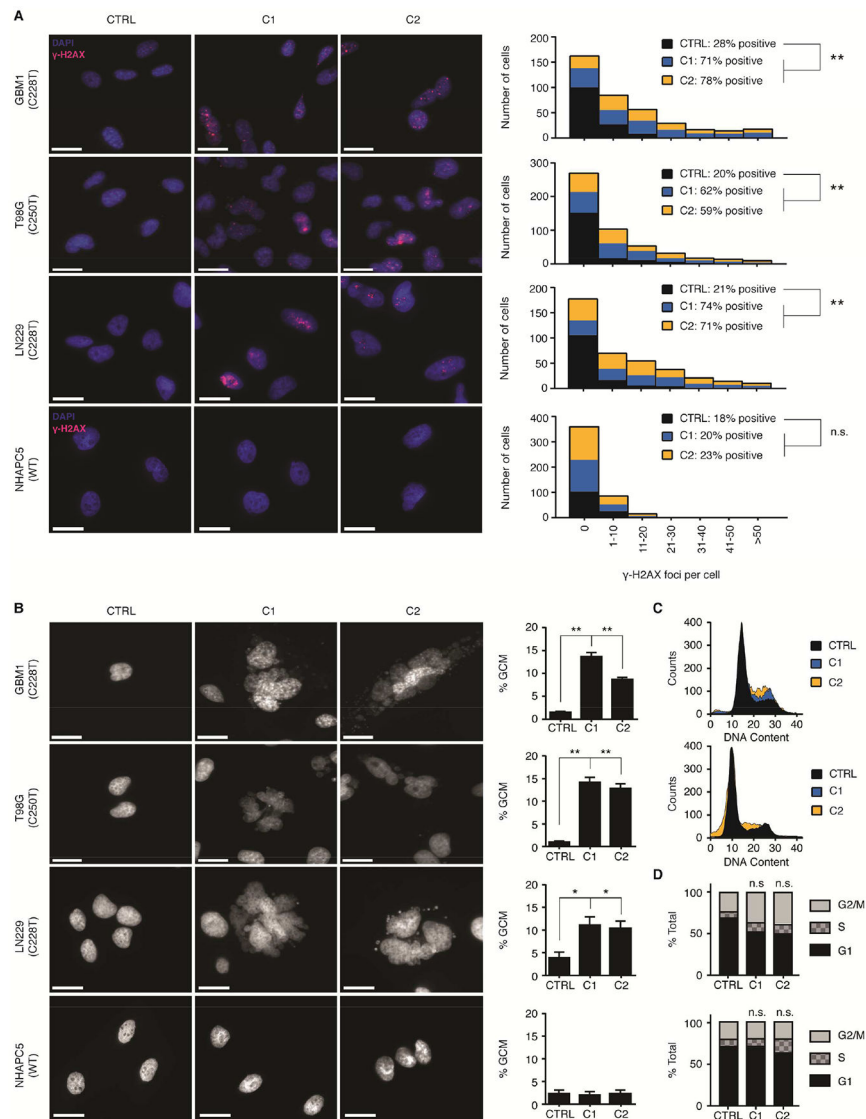


Figure 6. β 1L-reduced GBM lines accrue DNA damage and undergo mitotic cell death in a *TERT* promoter mutation-dependent manner. **(A)** Representative images (left images) and quantification (right graphs) of γ -H2AX staining in CTRL or β 1L-reduced clones at day 70–75 post-editing. Scale bar = 200 μ m. ***p* value < 0.01, two-sided Student's *t*-test compared to CTRL. Quantification values are sums of at least ten independent fields of view. **(B)** Representative DAPI images (left images) and quantification (right graphs) of giant cell micronucleation (GCM) in CTRL or β 1L-reduced clones at day 70–75 post-editing. Scale bar = 20 μ m. **p* value < 0.05, ***p* value < 0.01, two-sided Student's *t*-test compared to CTRL. Quantification values are weighted mean \pm S.D. of at least ten independent fields of view. **(C,D)** Histograms **(C)** and quantification **(D)** for cell cycle analysis of CTRL or β 1L-reduced LN229 (top graphs) and NHAPC5 (bottom graphs) lines at day 75 post-editing. See also Figures S6–S7 and Table S6.

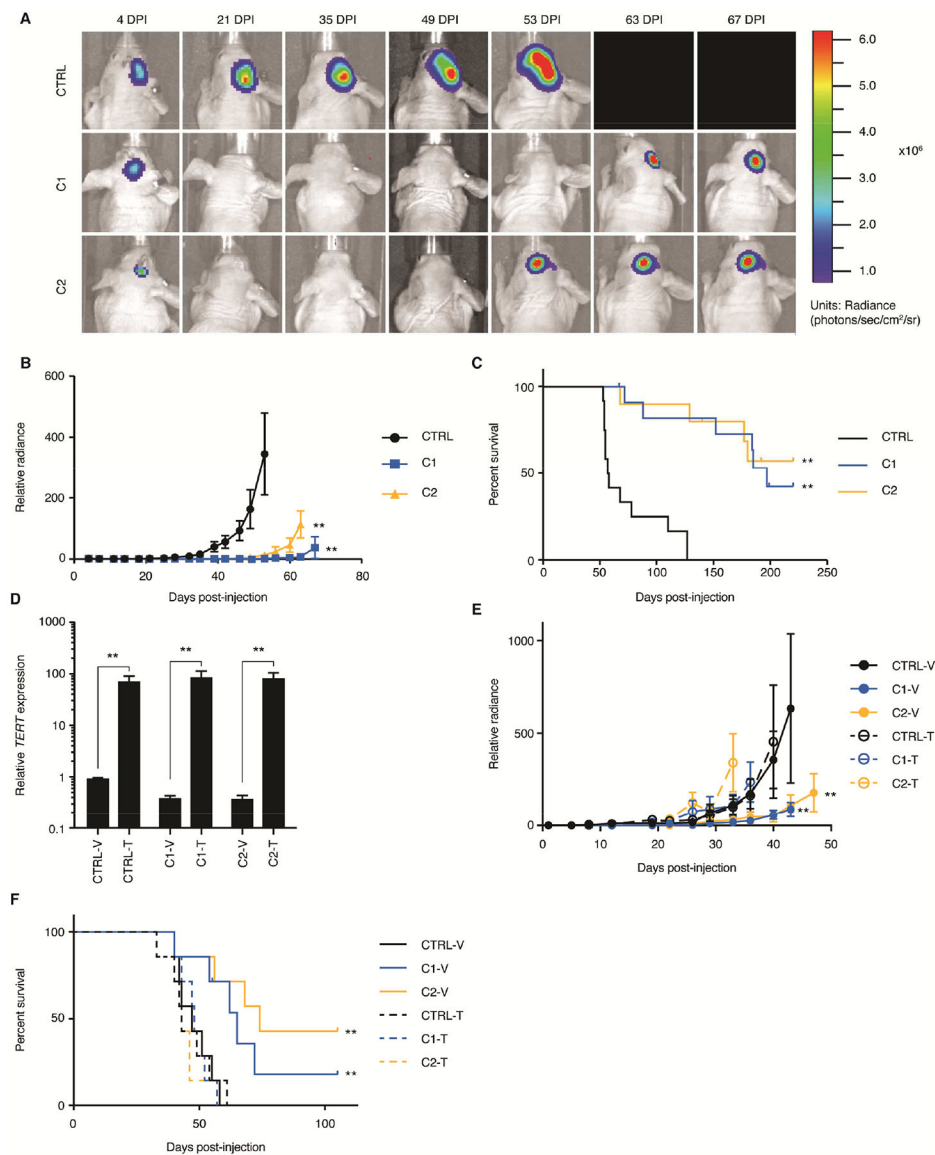


Figure 7. Reduction of $\beta 1L$ impairs tumor growth and extends mouse survival *in vivo*. **(A)** Representative IVIS bioluminescent images of CTRL or $\beta 1L$ -reduced LN229-derived tumors at 7 time points post-intracranial injection (injected on cellular day 51 post-editing). DPI = days post-injection. **(B)** Relative tumor bioluminescence quantified twice per week for each group (CTRL: n=12, C1: n=12, C2: n=10) until first recorded mortality. **p value<0.01, two-sided Student's t-test compared to CTRL peak luminescence. Values are mean \pm S.D of all mice in each group. **(C)** Kaplan-Meier survival curve displaying disease-specific survival of mice (Simonsen Labs, see STAR Methods) injected with LN229 CTRL or C1 and C2 $\beta 1L$ -reduced cells over time. **p value<0.01, log-rank test compared to CTRL. **(D)** *TERT* expression 4 days post-transduction of CTRL or $\beta 1L$ -reduced LN229 clones (41 days post-editing) with either a control (V) or TERT (T) lentiviral expression vector. **p value<0.01, two-sided Student's t-test relative to respective vector (V) control.

Values are mean \pm S.D of three independent experiments. **(E)** Relative tumor bioluminescence quantified twice per week for each group (n=7 mice per group) following stable transduction with a control (V) or TERT (T) lentiviral expression vector. **p value<0.01, two-sided Student's t-test compared to vector control peak luminescence for each respective line. Values are mean \pm S.D of all mice in each group. **(F)** Kaplan-Meier survival curve displaying disease-specific survival of mice (Envigo, see STAR Methods) injected with LN229 CTRL or C1 and C2 β 1L-reduced cells following stable transduction with a control (V) or TERT (T) lentiviral expression vector. **p value<0.01, log-rank test compared to CTRL.

Author Manuscript

Author Manuscript

Author Manuscript

Author Manuscript